

Northumbria Research Link

Citation: Zhao, Hangyue, Wang, Lei, Belwal, Tarun, Jiang, Yunhong, Li, Dong, Xu, Yanqun, Luo, Zisheng and Li, Li (2020) Chitosan-based melatonin bilayer coating for maintaining quality of fresh-cut products. *Carbohydrate Polymers*, 235. p. 115973. ISSN 0144-8617

Published by: Elsevier

URL: <https://doi.org/10.1016/j.carbpol.2020.115973> <<https://doi.org/10.1016/j.carbpol.2020.115973>>

This version was downloaded from Northumbria Research Link:
<http://nrl.northumbria.ac.uk/id/eprint/42209/>

Northumbria University has developed Northumbria Research Link (NRL) to enable users to access the University's research output. Copyright © and moral rights for items on NRL are retained by the individual author(s) and/or other copyright owners. Single copies of full items can be reproduced, displayed or performed, and given to third parties in any format or medium for personal research or study, educational, or not-for-profit purposes without prior permission or charge, provided the authors, title and full bibliographic details are given, as well as a hyperlink and/or URL to the original metadata page. The content must not be changed in any way. Full items must not be sold commercially in any format or medium without formal permission of the copyright holder. The full policy is available online: <http://nrl.northumbria.ac.uk/policies.html>

This document may differ from the final, published version of the research and has been made available online in accordance with publisher policies. To read and/or cite from the published version of the research, please visit the publisher's website (a subscription may be required.)



UniversityLibrary



Northumbria
University
NEWCASTLE

1 Chitosan-based melatonin bilayer coating for maintaining quality of fresh-cut products

2

3 Hangyue Zhao^a (zhy-156@163.com, ORCID: 0000-0003-0179-1484)

4

Lei Wang^a (wangley@zju.edu.cn, 0000-0002-6949-4489)

5

Tarun Belwal^a (tarungbpihed@gmail.com, ORCID: 0000-0003-0434-1956)

6

Yunhong Jiang^b (yunhongjiang@yahoo.com, ORCID: 0000-0003-3292-8164)

7

Dong Li^a (dong_li@zju.edu.cn, ORCID: 0000-0002-1800-1656)

8

Yanqun Xu^a (xuyanqun@zju.edu.cn, ORCID: 0000-0003-3488-9445)

9

Zisheng Luo^{a,c} (luozisheng@zju.edu.cn, ORCID: 0000-0001-8232-9739)

10

Li Li^{a,c,*} (lili1984@zju.edu.cn, ORCID: 0000-0002-1242-3866)

11

12 ^aKey Laboratory for Agro-Products Postharvest Handling of Ministry of Agriculture and
13 Rural Affairs, College of Biosystems Engineering and Food Science, Zhejiang University,
14 Hangzhou 310058, China

15 ^bBristol Dental School, University of Bristol, Bristol BS1 2LY, UK

16 ^cNingbo Research Institute, Zhejiang University, Ningbo 315100, China

17

18 *To whom correspondence should be addressed: Dr. Li Li (lili1984@zju.edu.cn; Telephone:
19 +86-571-88981885; Fax: +86-571-88981885.)

20

21 **Abstract**

22 This work was designed to develop the chitosan-based melatonin layer-by-layer assembly
23 (CMLLA) via the inclusion method and further to test the effectiveness on fresh produce.
24 The structural characterizations and interaction present in CMLLA were investigated by
25 the scanning electron microscope (SEM), X-ray diffraction (XRD) and Fourier
26 Transform-Infrared spectroscopy (FTIR). The ratio of chitosan (CH) to
27 carboxymethylcellulose (CMC) greatly influenced the mechanical properties, including the
28 tensile strength, moisture content and color performance. The antioxidant capacity of
29 CMLLA was determined by evaluating the scavenging effect and the antimicrobial activity
30 was evaluated using the zone of inhibition against infected bacterial. Results showed that
31 both antioxidant and antimicrobial properties of CMLLA were enhanced with the addition
32 of melatonin (MLT). Furthermore, the possible practical application of CMLLA as edible
33 coating on fresh products by was investigated. It was demonstrated that the CMLLA with
34 1.2% (w/v) CH, 0.8% (w/v) CMC and 50 mg/L MLT better contributed to the delay of
35 chlorophyll degradation and the maintenance of shelf-life quality. Results from this study
36 might open up new insights into the approaches of quality improvement of postharvest
37 fresh products by incorporating the natural antioxidant compounds into natural polymers.

38

39 **Keywords:**

40 Melatonin-loaded; assembly; layer by layer; structural property; antioxidant capacity,
41 antimicrobial activity

42

43 1. Introduction

44 The natural polysaccharides applied on packaging of fresh produces have increased
45 tremendously with more emphases on development of eco-packaging coating materials in
46 last few years (de Moraes Crizel et al., 2018; Medina-Jaramillo, Ochoa-Yepes, Bernal, &
47 Famá, 2017). The incorporated natural bioactive compounds in packaging films are of
48 great importance, which provides various functional properties to the films, such as
49 antioxidant, antimicrobial. The advantages of selecting natural compounds over synthetic
50 have well been reviewed and discussed over many years (Noronha, de Carvalho, Lino, &
51 Barreto, 2014; Sozer & Kokini, 2009; Song et al., 2018). For instance, the higher toxicity of
52 synthetic antioxidants was well explained and thus substituted by the natural antioxidants
53 (Noronha, de Carvalho, Lino, & Barreto, 2014; Huang et al., 2015; Park, Choi, Hu, & Lee,
54 2013; Tang et al., 2016).

55 Among various natural antioxidants, melatonin (MLT), a natural hormone that is primarily
56 released by the pineal gland to the blood circulation, exerts various biological activities
57 such as antioxidant, antimicrobial, and anti-apoptotic (Wang et al., 2018; Arnao and
58 Hernandez-Ruiz, 2018). In a recent study, MLT has been applied in preharvest and
59 postharvest fresh products due to the excellent antioxidant capacity (Sun et al., 2019; Tan
60 et al., 2007; Shi et al., 2015). For instance, Tan et al. (2007) reported that the improved
61 antioxidant capacity and tolerance to copper contamination in pea plants by exogenous
62 MLT (Tan et al., 2007). Moreover, MLT has been widely used to postpone chlorophyll
63 degradation of barley leaves (Arnao & Hernández-Ruiz, 2009), and to reduce oxidative
64 damage of grape cuttings (Meng et al., 2014). Considering the post-harvested products,
65 the application of MLT could effectively prolong the shelf-life and also maintain the
66 postharvest quality attributes (Tan et al., 2012; Liu et al., 2016). Furthermore, it was
67 demonstrated that exogenous MLT significantly reduced the weight loss and decay
68 incidence, as well as maintained firmness and total soluble solids of postharvest peach
69 (Gao et al., 2016). In a recent report, the application of MLT was found to be effectively
70 attenuate the fungal decay and maintain the nutritional quality of post-harvested
71 strawberry as well as trigger the accumulation of H₂O₂ accumulation, which resulted from
72 higher superoxide dismutase (SOD) activity (Aghdam et al., 2017). Overall, MLT
73 potentially contributed to maintaining quality in postharvest fresh-cut products. However,
74 the direct dose of MLT posed difficulties during the processing procedure as the low
75 solubility of MLT in water, while the antioxidant capacity of MLT was significantly affected.
76 Thus, the suitable delivery system loading MLT are essential to sustain and prolong its
77 efficiency, which is analogous to that used in drug and medical industry (Malafaya, Silva,
78 & Reis, 2007). Chitosan, a poly-*N*-acetyl-glucosaminoglycan obtained by alkaline
79 deacetylation of chitin, is an excellent coating material known for its outstanding film
80 forming properties with good mechanical performance and barrier capacity (Kurek,

81 Guinault, Voilley, Galić, & Debeaufort, 2014; Martins, Cerqueira, & Vicente, 2012).
82 Besides that, several studies showed that chitosan had inherent antibacterial and
83 antifungal properties, depends on its degree of deacetylation and molecular weight (Aider,
84 2010; Tan et al., 2015). In spite of the mechanical and antimicrobial properties,
85 nevertheless, the single chitosan film did not present ideal antioxidant capacity (Liu et al.,
86 2017). To meet out this challenge, various approaches have been tested for improving the
87 coating film quality for better packaging of fresh produce by incorporating the natural
88 antioxidant compounds, such as green tea extract and black soybean seed coat extract
89 (Wang et al., 2018; Rubilar et al., 2013; Siripatrawan & Harte, 2010). In addition, natural
90 antimicrobial agents have been used to develop the antimicrobial packages, including
91 plant extracts such as grapefruit seed extract (Wang, Lim, Tong, & Thian, 2019), and whey
92 protein (Brink, Šipailienė, & Leskauskaitė, 2019). As a natural biopolymer, chitosan was
93 incorporated directly into meat products to inhibit microbial growth and to increase
94 shelf-life of the meat products (Soultos, Tzikas, Abraham, Georgantelis, & Ambrosiadis,
95 2008). Besides, it is common to blended chitosan with other polymers to obtain better
96 packaging coating (van den Broek, Knoop, Kappen, & Boeriu, 2015). Recently, chitosan
97 nanoparticles were used in delivery system of food packaging extending shelf-life of food
98 (Lin, Xue, Duraiarasan, & Haiying, 2018). In this line, recently our group has introduced
99 the idea of developing layer-by-layer (LBL) assembly of chitosan and carboxymethyl
100 cellulose (CMC), which provide higher antioxidant and antimicrobial activities to the
101 packaging film for postharvest fresh produce (Yan et al., 2019).

102 Following and expanding research with similar idea and considering MLT as a natural
103 active antioxidant compound, the aim of the present work was to develop chitosan-based
104 melatonin layer-by-layer assembly (CMLLA) as an innovative and active melatonin film
105 formulation applicable to the post-harvested fresh products. Up to now, MLT-loaded
106 polysaccharides assembly films have not been formulated and tested for its active role in
107 fresh products. In the present study, the CMLLA was developed via the self-assembled
108 molecular technique. The structure, color, biological and mechanical properties of the
109 novel chitosan-based melatonin assembly were assessed. Further, to find the practical
110 applicability of the developed films, the effect of CMLLA on quality attributes of three
111 fresh-cut products were evaluated.

112 **2. Material and methods**

113 *2.1 Materials*

114 Food-grade chitosan (CH, deacetylation degree 91.0%) and carboxymethyl chitosan
115 (CMCH, deacetylation degree: 91.0%) were bought from Golden-shell Pharmaceutical
116 Co., Ltd, Zhejiang Province, and the carboxymethyl cellulose (CMC, viscosity:
117 800-1200mpa·s) was procured from Shanghai Aladdin Bio-Chem Technology Co., LTD

118 (Shanghai, China). Melatonin (MLT) (contains 10%-20% benzene, $\geq 97.0\%$ HPLC), Acetic
119 acid (98% HPLC), pure ethanol (95% HPLC) was purchased from Shanghai Aladdin
120 Bio-Chem Technology Co., LTD (Shanghai, China). The 2,2-diphenyl-1-picrylhydrazyl
121 (DPPH) was purchased from Sigma Chemical Co. (St. Louis, MO, USA). Deionized water
122 (Millipore) was used to prepare the solutions. All other reagents were of analytical grade.

123 *2.2 Preparation of CMLLA*

124 The CH solution was prepared by dissolving chitosan powder in a 1% (v/v) aqueous
125 acetic acid solution to obtain a chitosan concentration of 2.5% (w/v) in an assembly
126 system. The CMCH and CMC solutions were prepared separately by dissolving 2.5g of
127 each in 100 mL of deionized water to obtain the concentration of 2.5% (w/v) in an
128 assembly system. All the solutions were homogenized by magnetic stirring for 2 h at room
129 temperature until complete dissolution. To prepare the MLT-loaded assembly of CH,
130 CH-M25, CH-M50, and CH-M100, which means MLT was added to CH solution at
131 different concentrations of 0, 25, 50, 100 mg/L, respectively, and homogenized by
132 magnetically stirring for 10 min.

133 The simple CH, CMCH and CMC, as well as the CH/MLT, CMCH/MLT assemblies were
134 obtained by pouring the stock solutions into a glass dish. The solvents were removed by
135 drying in a ventilated climatic chamber at 27 °C and 50% RH for 24 h. The dried surface
136 was then peeled off and stored at 25°C and 53% RH until further analysis to obtain
137 corresponding CMLLA. The CMLLA was prepared based on difference ratios of
138 CH/CMCH to CMC stock solutions (1:4, 2:3, 3:2, and 4:1).

139 *2.3 Structural characterization*

140 The Fourier Transform-Infrared spectroscopy (FTIR) spectra of CMLLA were obtained
141 by AVATAR370 FT-IR (Thermo Nicolet, USA). The crystalline characteristics were
142 determined by X-pert powder diffractometer (Panalytical B.V., Netherland), which was
143 operated at 40 mA and 40 kV using Ni-filtered Cu K α radiation. The diffraction pattern was
144 obtained from 2θ , 5° to 80° at a scan rate of 0.1° per second. A scanning electron
145 microscope (SEM, HITACHI, Tokyo, Japan) was used to observe the cross-sectional
146 microstructures of the films. The accelerating voltage of the SEM was 200 kV. The films
147 were frozen with liquid nitrogen and pinched out with tweezers. The samples prepared
148 were then fixed on individual specimen stubs and sputter-coated with gold. The
149 cross-sectional photographs of the films were obtained at magnifications of 1000 \times and
150 10,000 \times , respectively.

151 *2.4 Physical characterization*

152 *2.4.1 Thickness*

153 The assembly thickness was measured by CHY-C2 Thickness Tester (PARM™, China).

154 The average values of five thickness measurements at different positions were used in all
155 calculations.

156 2.4.2 Color and opacity

157 The color was determined by the CR-400 Chroma Meter (Konica Minolta Sensing, Inc.,
158 Japan). The L*(lightness), a* (red to green) and b* (yellow to blue) values were averaged
159 from three readings for each sample. And then the total color difference (ΔE) was
160 calculated as per the equation (1) (Gennadios, Weller, Hanna, & Froning, 1996):

$$161 \quad \Delta E = \sqrt{\Delta L^{*2} + \Delta a^{*2} + \Delta b^{*2}} \quad \text{Eq. (1)}$$

162 where, ΔL^* , Δa^* and Δb^* are the differences between the color parameter of the
163 samples and those of the white standard ($L^*= 92.82$, $a^* = -1.24$, $b^* = 0.46$).

164 The opacity was determined by measuring the film absorbance at 600 nm, using
165 UV-5800PC spectrophotometer (METASH, China), following the method of Park et al.
166 (2004). The film opacity was calculated by the absorbance against the thickness. All
167 measurements were performed in triplicate.

168 2.4.3 Moisture content

169 CMLLA was cut into square pieces (20 mm × 15 mm) and the accurate weight (M_1) and
170 the constant weight (M_2) was calculated. The moisture content was determined by the
171 following equation (2):

$$172 \quad \text{Moisture content (\%)} = (M_1 - M_2) / M_2 \times 100\% \quad \text{Eq. (2)}$$

173 2.4.4 Mechanical properties

174 The tensile strength (TS, in MPa) and percentage of elongation at the breakpoint (E, %)
175 were determined by XLW (M) auto Tensile Tester (PARAM™, China), according to
176 American Society for Testing Material (ASTM) standard method D882 (ASTM, 1992).
177 Briefly, the assembly samples were cut into rectangular pieces (1 cm × 5 cm) and
178 mounted in the extension grips of the testing machine and stretched axially at a rate of 50
179 mm·min⁻¹. Three film specimens were used for each replicate.

180 2.5 *Biological activities*

181 2.5.1 Antioxidant capacity

182 The antioxidant capacity of the assembly was measured by DPPH radical scavenging
183 assay (Mayachiew, Devahastin, 2010). Briefly, the assembly sample was stirred and
184 dissolved in 10 ml of deionized water and mixed with DPPH reagent (150 μmol/L). The
185 absorbance was recorded at 517 nm for every 10 min in 2 h of reaction time. All
186 measurements were performed for three replications.

187 2.5.2 Antimicrobial property

188 The antimicrobial properties of CMLLA were examined by the zone of inhibition assay
189 on solid media as per the Seydim (2006) protocol with slight modifications. Three
190 bacteria, *Salmonella Enteritidis* (*S. enteritidis*, ATCC 13076), *Escherichia coli* (*E. coli*,
191 O157:H7, ATCC 35218), and *Listeria monocytogenes* (*L. monocytogenes*, NCTC 2167),
192 which commonly present in fresh-cut products based on previous study, were used in
193 antimicrobial assay (Fernandez-Saiz, Lagaron, & Ocio, 2009; Portes, Gardrat, Castellan,
194 & Coma, 2009; Sánchez-González, González-Martínez, Chiralt, & Cháfer, 2010). Briefly,
195 every 100 µL of bacterial cultures (colony count of 1×10^8 CFU mL⁻¹) inoculated in 10 mL of
196 molten LB nutrition agar. Test discs were placed on the bacterial lawns. The plates were
197 incubated at 37°C for 24 h. The diameter of the test discs was 10mm. The diameter of the
198 zone of inhibition was measured with a caliper. The average value of the zone of inhibition
199 was calculated as the means of three measurements.

200 2.6 CMLLA on quality traits of fresh produce

201 Fresh produce of *Cucumis sativus* (cucumber), *Brassica oleracea* (broccoli) and
202 *Cucumis melo* (melon) in uniform color and size without mechanical injury were selected
203 and cut into ready-to-eat pieces and subjected to different treatments (control (pure water),
204 According to the previous study of Yan et al. (2019), the control group was immersed in
205 distilled water for 30 s, the single layer group was immersed in the 1.2% CH/CMCH
206 solution for 30 s, and the CMLLA group was first coated with CH/CMCH solution under
207 different concentration and dried at room temperature for 20-30 min, and then coated with
208 CMC (Table 1). After the produce surface was completely dry, all samples placed in the
209 plastic casing at room temperature Based on the properties of fresh products and
210 Accelerated Shelf-life Test (ASLT), storage time was 5 days for cucumber, 7 days for
211 broccoli and 5 days for melon, respectively, All quality attributes below were determined
212 for three technical replications and three biological replications. The weight loss of the
213 ready-to-eat produce was calculated by comparing the initial and final weight (Sathivel,
214 2005). The firmness was measured using a TA-XT2i texture analyzer (Stable
215 Microsystems Texture Technologies Inc., UK) with a cylindrical probe (5 mm diameter)
216 with the test speed of 0.5 mm s⁻¹ and a pierce distance of 5 mm. Firmness was tested at
217 three locations on each fruit and the result was expressed as the maximum compression
218 force (g). The content of titratable acidity (TA) and total soluble solids (TSS) was
219 measured using a PLA-1 pocket refractometer (ATAGO CO., Tokyo, Japan). The juice
220 from fruit samples was squeezed out and used immediately for determining TA and TSS
221 concentration. The color of the ready-to-eat produce was determined by CR-400 Chroma
222 Meter (Konica Minolta Sensing, Inc., Japan). Furthermore, the chlorophyll content in
223 broccoli was measured by recording the absorbance at 663 nm and 645 nm using a
224 UV-5800PC spectrophotometer (METASH, China).

225 **Table 1.** Assembly with different components in the present study.

Assembly	Addition of components		
	CH/CMCH (%)	CMC (%)	MLT (mg/L)
Control	0	0	0
CH/CMCH	1.2	0	0
CH-M25	2.4	1.6	25
CH-M50	2.4	1.6	50
CH-M100	2.4	1.6	100
CH/CMCH1.2	1.2	0.8	50
CH/CMCH1.8	1.8	1.2	50
CH/CMCH2.4	2.4	1.6	50

226 2.7 Statistical analysis

227 The results were analyzed by the statistical software SPSS ver. 18.0 (SPSS Inc.,
 228 Chicago, IL, USA). All data was expressed as means \pm standard deviations (SD) from
 229 three technical and biological replications. One-way analysis of variance (ANOVA) with a
 230 95% confidence interval of the data was conducted using SPSS 18.0 (SPSS Inc., Chicago,
 231 IL, USA).

232

233 3 Results and discussion

234 3.1 Structural Characterization

235 3.1.1. FTIR analysis

236 FTIR spectroscopy was carried out to demonstrate the interactions between CH/CMCH
 237 and CMC. In this study, three represented samples are shown to demonstrate the
 238 structure of CMLLA. Fig. 1 showed the FTIR spectra for the CH, CMCH, CMC, CH-CMC
 239 (3:2) and CMCH-CMC (3:2) assemblies.

240 The main bands observed in the CH spectrum (Fig. 1) were: (i) a broad asymmetric band
 241 between 3400 and 2500 cm^{-1} corresponding to the axial stretching of C-H bonds; (ii) a
 242 region between 1700-1200 cm^{-1} attributed to the amide groups; (iii) a strong absorption
 243 region between 1200-800 cm^{-1} due to the polysaccharide skeleton, including the vibration
 244 of the glycoside bonds, C-O and C-O-C stretching (Zhai et al., 2017; Branca et al., 2016;
 245 de Abreu & Campana-Filho, 2009; Wang et al., 2005). It was demonstrated in Fig. 1 that
 246 the structural difference between the CH spectrum and the carboxymethylated CMCH, (i)
 247 the broader band centered at 3300 cm^{-1} which revealed the more hydrophilic
 248 characterization of CMCH; (ii) the presence of an intense band in 1630 cm^{-1} and a
 249 moderate band at 1423 cm^{-1} , were contributed to the symmetric and asymmetric axial

250 deformation of COO, respectively (Bao et al., 2014; de Abreu & Campana-Filho, 2009;
251 Esteghlal, Niakousari, & Hosseini, 2018). In the CMC spectrum, the characteristic bands
252 in 3423 cm^{-1} and 2921 cm^{-1} were assigned to -OH and -CH stretching regions,
253 respectively (Fig. 1). The characteristic absorption bands of symmetric and asymmetric
254 -COO were observed in 1418 cm^{-1} and 1605 cm^{-1} , respectively. These characteristic
255 absorption bands are consistent with that in previous studies (Esteghlal, Niakousari, &
256 Hosseini, 2018).

257 In the spectrum of CH-CMC sample (Fig. 1), the region between 3400 and 2000 cm^{-1}
258 with a clear increase in the intensity of the bands, indicating the amino proton was
259 synthesized to be NH_3^+ in the film. The band of N-H stretching vibration was shifted to
260 3420 cm^{-1} , indicate hydrogen bond association. The C=O and N-H groups were
261 overlapped with a shift of C-O stretching vibration to 1410 cm^{-1} , showed the existence of
262 COO^- , indicating the intermolecular hydrogen bonding of $\text{C=O}\dots\text{H-N}$ between two
263 materials. The peak of C-H at 2926 cm^{-1} became weaker, attributing to the intermolecular
264 interaction between CH and CMC (Boy et al., 2016). In the CMCH-CMC spectrum, the
265 overlapped bands at 1581 cm^{-1} are associated with the asymmetric stretching of
266 carboxylic anion COO^- and the stretching of the amino group. The absorption at 1065 cm^{-1}
267 attributed to C-O-C pyranose ring vibration in CMCH and CMC (Esteghlal, Niakousari, &
268 Hosseini, 2018; Yang, Yan, Chen, Lee, & Zheng, 2007). Besides, the peak of amide III
269 in the spectrum of CMC-CMCH film at 1322 cm^{-1} of C-H became weaker, indicating a
270 replacement of the amino group and these results indicated the presence of heterocyclic
271 amine and ester bond in CMLLA.

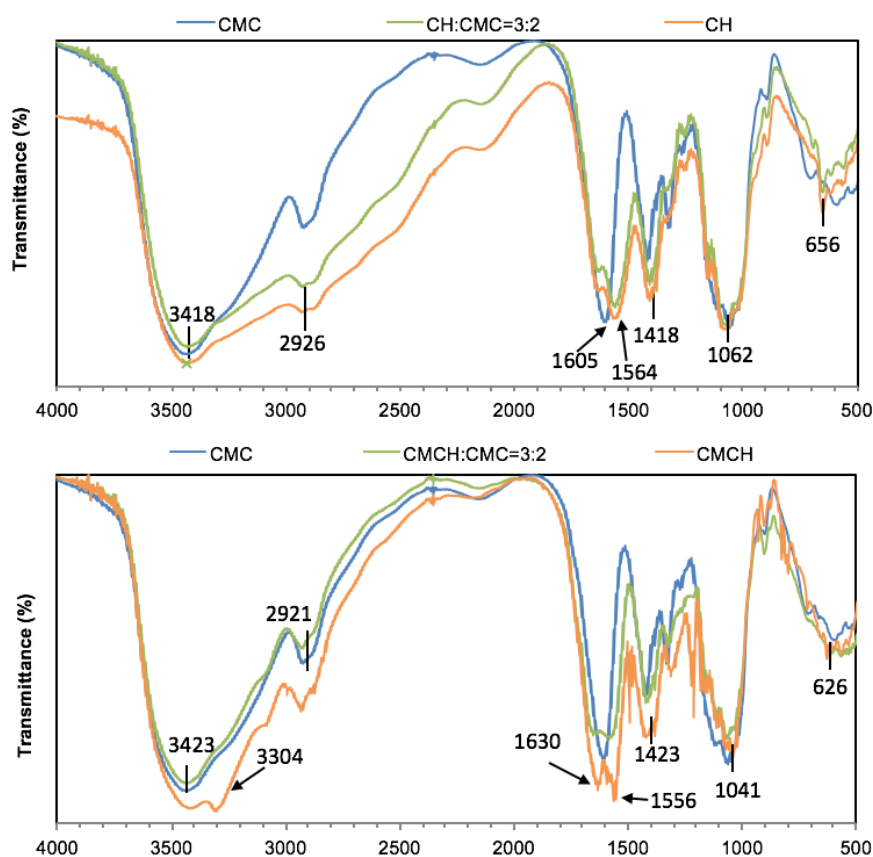


Fig. 1. FT-IR spectra of CMLLA films. (a) CH/MLT-CMC; (b) CMCH/MLT-CMC

3.1.2. XRD patterns

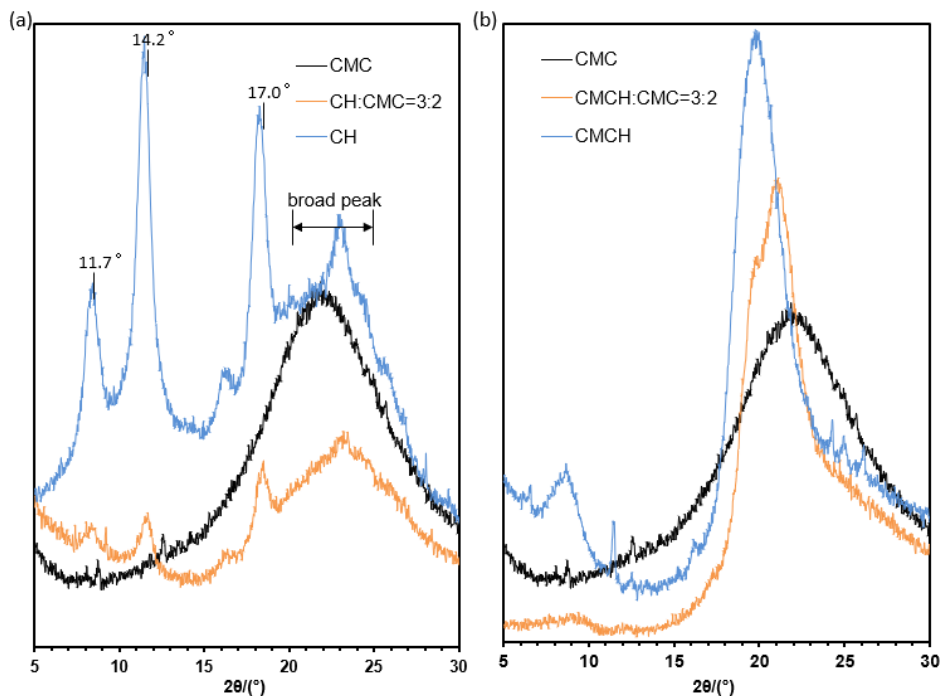
Crystalline characteristics of CMLLA were determined by XRD. As shown in Fig. 2, the simple chitosan film presented a semi-crystalline characteristic with diffraction peaks at 11.7° , 14.2° and 17.0° , which were similar to the previous studies (Liu et al., 2017; Tan et al., 2015). The diffraction peak at 11.4° was owing to the hydrated crystalline structure, while the broad peak at 20° - 23° represented the amorphous structure of chitosan (Rivero et al., 2010). Compared with CH, the spectrum of CMCH exhibited poorly defined and less intense peaks, which was resulted from the presence of carboxymethyl groups substituting the hydrogen atoms of the hydroxyl and amino groups (de Abreu & Campana-Filho, 2009).

When incorporated with CMC into the CMLLA, the broad peak became wider and weaker. It was demonstrated that the overall crystallization rate was low, as the intensity of the crystal peak of CH at 20° (2θ) declined significantly, compared to CH. Furthermore, it was proved that the molecular chains of both crystalline polymers without presence of crystallization, of which the domains of both components were scarcely formed (Sakurai et al., 2000). Therefore, the amorphous nature of the CMLLA further confirmed the good miscibility of the components. This was probably due to the intermolecular interaction between hydroxyl groups and NH_3^+ in CMC and chitosan, which limited the molecular

292 movement of both chitosan and CMC (Mathew & Abraham, 2008; Liu et al., 2016). These
293 results further strongly predicted the good compatibility of two constituents in CMLLA.
294 Presence of CMC induced the looseness of chitosan structure, resulting in a matrix more
295 unlikely to hydrogen bonding formation and leading to the decrease of the crystallinity.

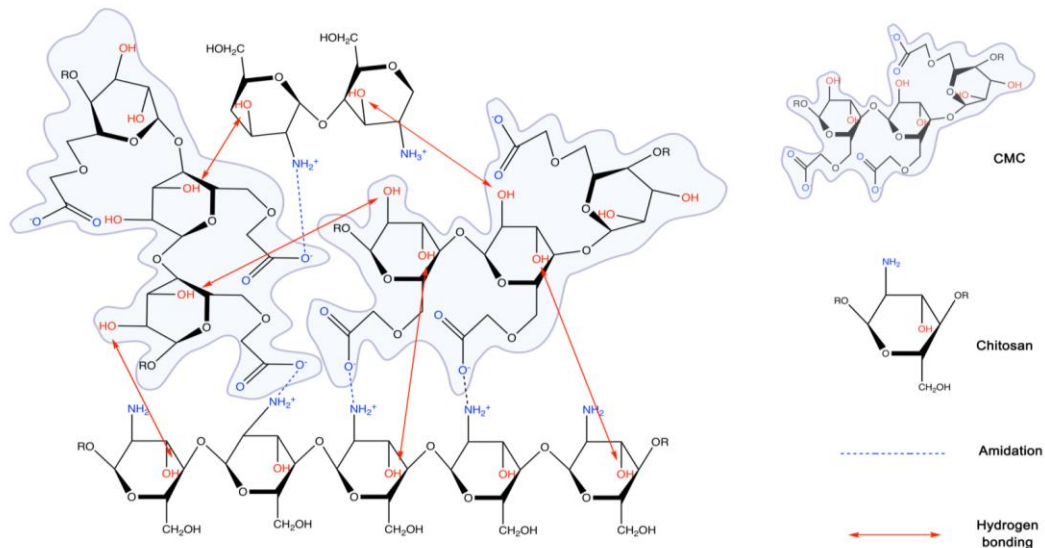
296 Block backbone model was built to illustrate the tentative interaction mechanisms
297 between CH and CMC (Fig. 3). The model showed that the two components would have
298 hydrogen bonding and amidation to form a complex network. The OH group of CMC
299 molecules interacted with OH groups of chitosan, leading to a matrix less favorable to
300 hydrogen bonding with water which in turn would decrease moisture content of CMLLA. In
301 the model, there are C=O...H-N intermolecular hydrogen bonding between two materials.
302 Therefore, compared to the molecular distance of simple chitosan film, CMLLA showed
303 obvious differences and the latter might be slightly looser than the former (Feng, Liu, Zhao,
304 & Hu, 2012; Okuyama et al., 2000). The much loose arrangement of CMLLA might
305 facilitate the penetration of water molecules.

306



307

308 **Fig. 2.** XRD patterns of CMLLA films. (a) CH/MLT-CMC; (b) CMCH/MLT-CMC



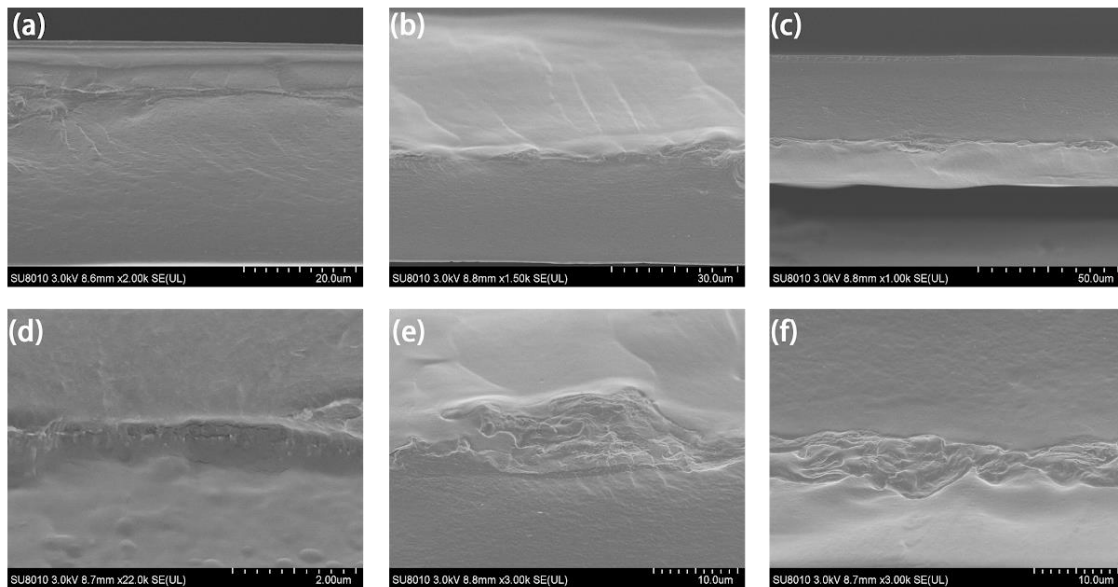
309

310 **Fig. 3.** The built block backbone model to illustrate the tentative interactions between CH
 311 and CMC.

312

313 3.1.3. Microstructural analysis

314 The microstructure of cross-section of CMLLA was investigated by SEM. Fig. 4 showed
 315 the microstructure of cross-section of the film (CH:CMC = 1:4, 2:3, 3:2) which can provide
 316 information about different components and interaction between two constituents. The
 317 surface of the plain chitosan film showed a smooth and uniform appearance (Fig. 4a). The
 318 intersection of CH-CMC film appeared somewhat rough (Fig. 4d), which may be due to
 319 the interaction between chitosan and CMC. In previous studies, similar results were
 320 reported which showed chitosan-Sodium alginate (SA) films had rough surface between
 321 intersection which indicated less homogeneity of the components owing to the positive
 322 and negative charged interactions (Li et al., 2019; Sogut, & Seydim, 2018). The film's
 323 morphologies had an obvious difference compared to the different ratio of film's
 324 constituents (Fig. 4). Among all the films tested, film (CH:CMC=1:4, 2:3) had obvious
 325 fracture surface in the intersection (Fig. 4d, e), while film (CH:CMC=3:2) was more
 326 uniform and smooth (Fig. 4f), probably due to the interaction between chitosan and CMC.
 327 In the study of Sogut et al. (2018), the addition of nano-cellulose (NC) into CH up to 10%
 328 resulted in a smooth surface in the cross-section of the bilayer films, which can effectively
 329 enhance the properties of CH due to the similarity of cellulose CH (Khan, Huq, Khan,
 330 Riedl, & Lacroix, 2014).



331

332

Fig. 4. Scanning electron microscope images of CH:CMC=1:4 at 1,500× (a) and 220,000× (d) magnification, CH:CMC=2:3 at 1,000× (b) and 10,000× (e) magnification, and CH:CMC=3:2 at 1,000× (c) and 10,000× (f) magnification.

333

334

335

336

3.2 Physical characterization

337

3.2.1 Opacity and color

338

339

340

341

342

343

344

345

346

347

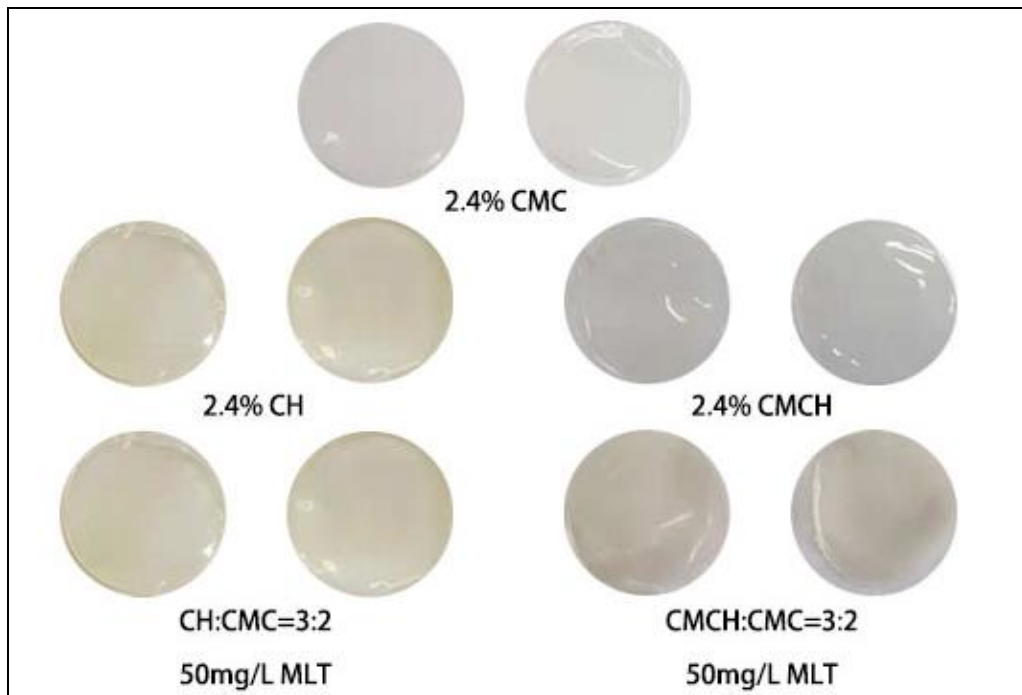
348

349

350

351

Color is an important property of assembly appearance. Assembly with different ratio of chitosan and CMC were prepared to verify color changes of samples. Fig. 5 showed the morphology and visible color variation of CMLLA. Color and opacity parameters of films were summarized in Table 1. Results showed that bilayers under different ratio had a significant distinction in color and opacity ($p<0.05$). The film color was visibly changed from pale white with low opacity for CMC film to yellow for CH, and high opacity for CMCH, respectively (Fig. 5). The color of pure chitosan was associated with the carotenoid pigment astaxanthin (Kucukgulmez et al., 2011) and the preparation procedure (Seo, King, & Prinyawiwatkul, 2007). The color difference increased with the increasing ratio of chitosan, with ΔE ranging from 8.24 for the assembly (CH:CMC = 1:4) to 12.10 for the assembly (CH:CMC = 5:0). However, the increased ratio of chitosan had little influence on the opacity of assembly. In CMCH-CMC assembly, the opacity significantly increased when the ratio of CMCH increased ($p<0.05$).



352
353 **Fig. 5.** Morphology of CMLLA samples.
354

355 3.2.2 Mechanical properties

356 The mechanical properties of CMLLA included tensile strength (*TS*), elongation at break
357 (*E*), thickness (*T*), and moisture content (*MC*) were shown in Table 1.

358 CH had the lowest *TS* (54.42 ± 3.67 MPa) and this value increased with the increasing
359 CMC concentration, which increased twice than the simple CH. Similarly, reports indicated
360 that when CH was combined with CMC, the *TS* increased by 150% (Marzieh, 2019). In the
361 previous research from Zhuang et al. (2018), nevertheless, the mechanical strength of
362 LBL assembly was 38.27% lower than that of single-layer sodium alginate (SA), which
363 probably due to the materials of the bilayers that had bad compatibility with each other. On
364 the contrary, simple CH has higher *E* value, while the combination with CMC would
365 decrease the *E* value, which might be caused by the entanglement and interaction
366 between two polymer constituents. It has been proved that the mechanical behaviors had
367 a close relationship with the inner structure (Wu et al., 2016). Results of the present study
368 showed that CH-CMC assembly exhibited higher *TS* and lower *E* values which might be
369 owing to the hydrogen bonding and electrostatic interaction between the positively
370 charged CH and negatively charged CMC (Fig. 3).

371 The thickness of CMLLA is given in Table 1. As expected, CMLLA exhibited higher
372 thicknesses than simple chitosan and CMC films; and the average thickness of films
373 increased gradually with the increase in the ratio of chitosan. The average thickness of
374 CMLLA (CH:CMC = 4:1) was $75.3 \mu\text{m}$, which was 1.91 times thicker than simple CMC film.
375 This might be due to the intersection of CH and CMC, which can be also seen in SEM

376 images (Fig. 4).

377 The moisture content (*MC*) of CMLLA was shown in Table 1. It was widely suggested
378 that the higher *MC* of simple chitosan film was due to the strong hydrogen bond
379 interactions with water molecules (Aljawish et al., 2016). *MC* of assemblies reduced from
380 15.72% to 12.68%, when the ratio of chitosan increased from 0% to 40%. Compared with
381 simple chitosan and CMC, CH-CMC assemblies exhibited lower moisture contents which
382 might be owing to the hydroxyl and carboxyl groups in CMC molecules which interact with
383 the hydrophilic groups in chitosan (Marzieh et al., 2019). It was revealed that the CMLLA
384 (CH:CMC = 3:2) exhibited the best physical properties compared with other samples.
385 CH-CMC assembly maintained better mechanical properties with average thickness of
386 69.8 μm for CH and 56.1 μm for CMCH, and the opacity significantly as the CH ratio
387 increased ($p < 0.05$).

388 **Table 2.** Mechanical properties (*T*, Thickness, *E*, Elongation at break, *TS*, Tensile strength, *MC*, Moisture content), opacity and color changes (ΔE) of
 389 CMLLA films (average \pm standard deviation).

	CH						CMCH					
	<i>T</i> (μm)	<i>E</i> (%)	<i>TS</i> (MPa)	<i>MC</i> (% H ₂ O)	ΔE	Opacity	<i>T</i> (μm)	<i>E</i> (%)	<i>TS</i> (MPa)	<i>MC</i> (% H ₂ O)	ΔE	Opacity
0:5 [#]	39.4 \pm 3.4 ^{a*}	1.90 \pm 0.013 ^a	64.91 \pm 20.31 ^b	13.97 \pm 0.03 ^{ab}	6.98 \pm 0.12 ^a	1.452 \pm 0.030 ^a	39.4 \pm 3.4 ^a	1.90 \pm 0.013 ^a	64.91 \pm 20.31 ^b	13.97 \pm 0.03 ^a	6.98 \pm 0.12 ^a	1.452 \pm 0.030 ^a
1:4	54.4 \pm 3.1 ^b	1.90 \pm 0.013 ^a	52.27 \pm 6.67 ^a	16.31 \pm 0.01 ^b	8.24 \pm 0.31 ^a	1.225 \pm 0.337 ^a	39.1 \pm 7.3 ^a	5.71 \pm 0.040 ^{ab}	42.75 \pm 5.94 ^{ab}	15.63 \pm 0.01 ^a	8.00 \pm 0.06 ^b	1.422 \pm 0.176 ^a
2:3	66.7 \pm 10.8 ^{bc}	3.81 \pm 0.013 ^{ab}	58.91 \pm 5.63 ^a	12.68 \pm 0.01 ^a	9.78 \pm 0.66 ^b	1.407 \pm 0.162 ^a	48.1 \pm 4.3 ^{ab}	1.90 \pm 0.013 ^a	55.81 \pm 15.95 ^{ab}	12.65 \pm 0.02 ^a	8.36 \pm 0.46 ^{bc}	1.909 \pm 0.642 ^a
3:2	69.8 \pm 8.4 ^c	8.57 \pm 0.040 ^b	48.38 \pm 1.48 ^a	15.58 \pm 0.01 ^b	10.13 \pm 0.45 ^b	2.143 \pm 0.282 ^{ab}	56.1 \pm 3.4 ^b	7.62 \pm 0.013 ^b	43.41 \pm 5.20 ^{ab}	15.10 \pm 0.01 ^a	8.79 \pm 0.30 ^c	6.802 \pm 1.114 ^b
4:1	75.3 \pm 8.4 ^c	2.86 \pm 0.00 ^a	60.36 \pm 9.23 ^{ab}	14.11 \pm 0.01 ^{ab}	11.58 \pm 1.26 ^c	2.279 \pm 0.259 ^b	62.5 \pm 13.6 ^b	6.67 \pm 0.013 ^{ab}	44.55 \pm 0.56 ^{ab}	14.51 \pm 0.01 ^a	10.21 \pm 0.19 ^d	8.243 \pm 0.980 ^c
5:0	57.7 \pm 9.6 ^b	3.81 \pm 0.013 ^{ab}	54.42 \pm 3.67 ^a	15.72 \pm 0.00 ^b	12.10 \pm 1.48 ^c	1.274 \pm 0.145 ^a	46.7 \pm 7.0 ^a	10.48 \pm 0.049 ^b	34.49 \pm 10.25 ^a	16.46 \pm 0.04 ^{ab}	10.67 \pm 0.66 ^d	12.384 \pm 1.620 ^d

[#]Different proportion means the ratio of CH/CMCH and CMC.

*Different superscripts (a-d) within a column indicate significant differences among samples (p<0.05)

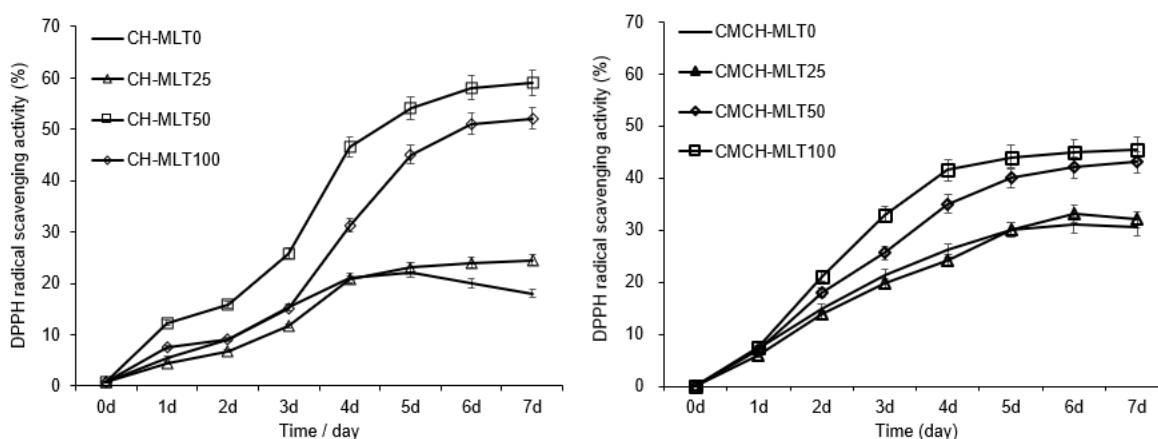
390 3.3 Biological activities

391 3.3.1 Antioxidant capacity

392 The free radical scavenging ability of the packaging films is usually required for active
393 packaging of fresh produce. The DPPH antioxidant activity of CMLLA was shown in Fig. 6.
394 The addition of MLT significantly increased the antioxidant capacity of CH-CMC assembly.
395 Compared with single chitosan film, the DPPH radical scavenging activity increased with
396 increasing of loaded MLT concentration and release time in assemblies. Nevertheless, the
397 DPPH radical scavenging activity of CH-MLT50 and CMCH-MLT50 were 45.55% and
398 30.67%, respectively. The result showed the higher antioxidant activity in CH film which
399 was different from previous studies (Guo et al., 2005; Zhao, Huang, Hu, Mao, & Mei, 2011;
400 Chen et al., 2015). The difference of antioxidant capacity was resulted from the different
401 solvent used for preparation of MLT stock solution. The introduction of carboxymethyl
402 groups into the chitosan, could increase the hydrogen-donating ability which actively
403 scavenged the DPPH radicals (Chen, & Ho, 1995; Zhao, Huang, Hu, Mao, & Mei, 2011)
404 (Lee, 2016). Compared with chitosan, CMCH had the significantly improved antioxidant
405 capacity, which probably due to the modified structure of CMCH. Moreover, the control
406 samples were shown the lower DPPH scavenging activity, which was consistent with that
407 in previous studies (Sun et al., 2017; Yen, Yang, & Mau, 2008). The exogenous addition of
408 MLT significantly increased the antioxidant capacity of CH/CMCH-CMC assembly. And the
409 antioxidant capacity of CH-MLT50 and CMCH-MLT100 increased by 2 folds compared to
410 the control. Moreover, the DPPH radical scavenging activity of CH-MLT50 and
411 CMCH-MLT50 were 45.55% and 30.67%, respectively.

412 Moreover, the study presented that antioxidant capacity increased slowly at first,
413 nevertheless, there was a significant difference between assemblies with or without
414 addition of MLT ($p < 0.05$). It was probably due to the viscosity of CH/CMCH, which leads to
415 the controlled release of MLT.

416



417

418 Fig. 6. Antioxidant capacity of CMLLA incorporated with different concentration of

419 melatonin.

420 CH, CH: CMC=3:2, CMCH, CMCH: CMC=3:2, MLT0, C_{MLT}=0 mg/L, MLT25, C_{MLT} =25
421 mg/L; MLT50, C_{MLT} =50 mg/L; MLT100, C_{MLT} =100 mg/L.

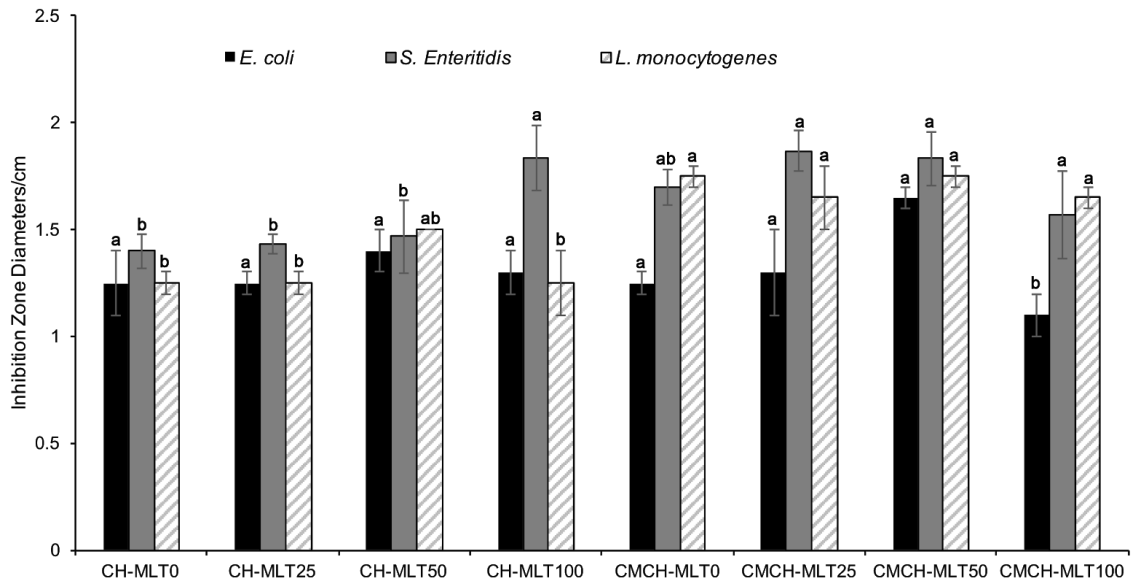
422

423 3.3.2 Antibacterial property

424 The zone of inhibition assay was employed to investigate the antibacterial property of
425 CH/MLT and CMCH/MLT assemblies against *S. enteritidis*, *E. coli*, and *L. monocytogenes*.
426 The inhibitory effect of CMLLA on the growth of three kinds of microorganisms was shown
427 in Fig. 7. Results revealed that there was little difference in inhibition zones between
428 control and MLT23. These results indicated the original antimicrobial property of CH and
429 CMCH. Consistently, Fernández-Saiz et al. (2013) also observed that chitosan could
430 inhibit the microbial growth in hake fillets when packaged in air and under vacuum. The
431 bacterial activity of CH might be owing to the free amino groups and the electrostatic
432 interaction. Binding to cell surface, disturbing the cell membrane, the amino groups may
433 cause the cell death by inducing leakage of intracellular components (Chung & Chen,
434 2008; Wahid et al., 2016). According to the study of Sayari et al. (2016), generally, the
435 chitosan exhibited higher antimicrobial activities on gram-positive bacteria than that on
436 gram-negative bacteria, which leading to the discrepancy of inhibition zone. And the order
437 of the antimicrobial activities of CMLLA against microorganisms was: *E. coli* < *L.*
438 *monocytogenes* < *S. enteritidis*, which was consistent with that in previous study (Jeon,
439 2001; Sun et al., 2017).

440 Furthermore, the MLT loading in the CMLLA delivery system increased the antibacterial
441 activity. It has been widely proved the antibacterial effect of MLT against gram-positive
442 and gram-negative bacteria, which ascribed to its ability to reduce intracellular substrates
443 availability such as free iron and fatty acids (Romić et al., 2016), although most research
444 of MLT was limited in the clinical study relevant to wound healing (Tekbas, Ogur, Korkmaz,
445 Kilic, & Reiter, 2008; Vielma et al., 2014). Our study showed that exogenous MLT may
446 effectively inhibit the growth of three presentative microorganisms. The inhibition zone of
447 CH-MLT100 against *S. enteritidis* was 1.83 cm, which was 1.31 times larger than that of
448 control (Fig. 7). All above results provided evidence that the antimicrobial activities of
449 CMLLA resulted from the synergic application of both CH and MLT. Result of the positively
450 antimicrobial properties indicated that the CMLLA could potentially be applied as
451 antimicrobial packaging materials in maintenance of quality attributes.

452



453
454 **Fig. 7.** Antibacterial activity of CMLLA samples.

455 CH, CH: CMC=3:2, CMCH, CMCH: CMC=3:2, MLT0, C_{MLT}=0 mg/L, MLT25, C_{MLT} =25
456 mg/L; MLT50, C_{MLT} =50 mg/L; MLT100, C_{MLT} =100 mg/L.

457
458 **3.4 CMLLA on quality traits of fresh produce**

459 **3.4.1 Cucumber (*Cucumis sativus*)**

460 Morphological characteristics of cucumber was exhibited in Fig. 8. As expected, the
461 surface of cucumber coated by CH was much whiter and rougher than control. And CMCH
462 coating contributed to the smooth and opaque morphology. Moreover, CMLLA better
463 maintained the appearance (Fig. 8a). The quality attributes of cucumber in response to
464 MLT-incorporated assembly were shown in Table a. Firmness was improved by 1.67 times
465 by CH1.2 than control, while in CMCH2.4 the firmness was 21.40% lower than control.
466 During postharvest storage, the sugar-acid ratio of cucumber decreased gradually. In
467 comparison to control, LBL coating significantly prevent the decrease in sugar-acid ratio,
468 which was 1.58 in CH1.2 group, and about 41.07% higher than control. And ΔE (Table 2)
469 showed that CH1.2 had minimal variation which was 57.2% lower than control.

470 Results revealed that CMCH (14.35%) had much more weight loss than CH (10.80%),
471 which might be due to the water solubility of CMCH that increase the loss of water on the
472 surface of cucumber produce. And compared with CH, CMCH increased the sugar
473 content by 9.1%. Furthermore, the viscosity of high concentration of CH and CMCH
474 applied in assembly contributed to the decrease of the oxygen and water vapor
475 permeability, and then accelerated the decomposition rate of the post-harvested
476 cucumber. The incorporation of loaded MLT would largely retain the sugar, firmness and
477 color in cucumber, which was consistent with the research reported by Xin et al. (2017),
478 where the cucumber was treated by MLT-incorporated assembly. Results revealed that

479 MLT could effectively better maintain the sensory properties of postharvest *Cucumis*
480 *sativus* and retard the decrease of TA, which indicated the better-quality maintenance of
481 the MLT loaded films.

482

483 3.4.2 Broccoli (*Brassica oleracea*)

484 Morphological characteristics of broccoli were presented in Fig. 8b. Compared with the
485 control group, the color of broccoli florets was much brighter and much greener when
486 coated with MLT film. However, the effect of MLT was suppressed when incorporated with
487 CH under high concentration, which accelerated the decline in the quality of broccoli,
488 along with increased bacterium infection and yellowing problem. The quality attributes of
489 broccoli were shown in Table 2. During postharvest storage, LBL coating dramatically
490 retards the decrease of firmness and weight. The firmness of low concentration (1.2%,
491 1.8%) of CH is 1.51 and 1.33 times harder than control. The weight loss of CH1.2 was
492 only 12.89%, which represent 42.89% lower than that of control. Furthermore, the results
493 of high concentration coating of broccoli were similar as for cucumber. There is no
494 difference in weight loss between control and CH2.4, however the color change of CH2.4
495 ($\Delta E=9.95$) increased significantly ($p<0.05$).

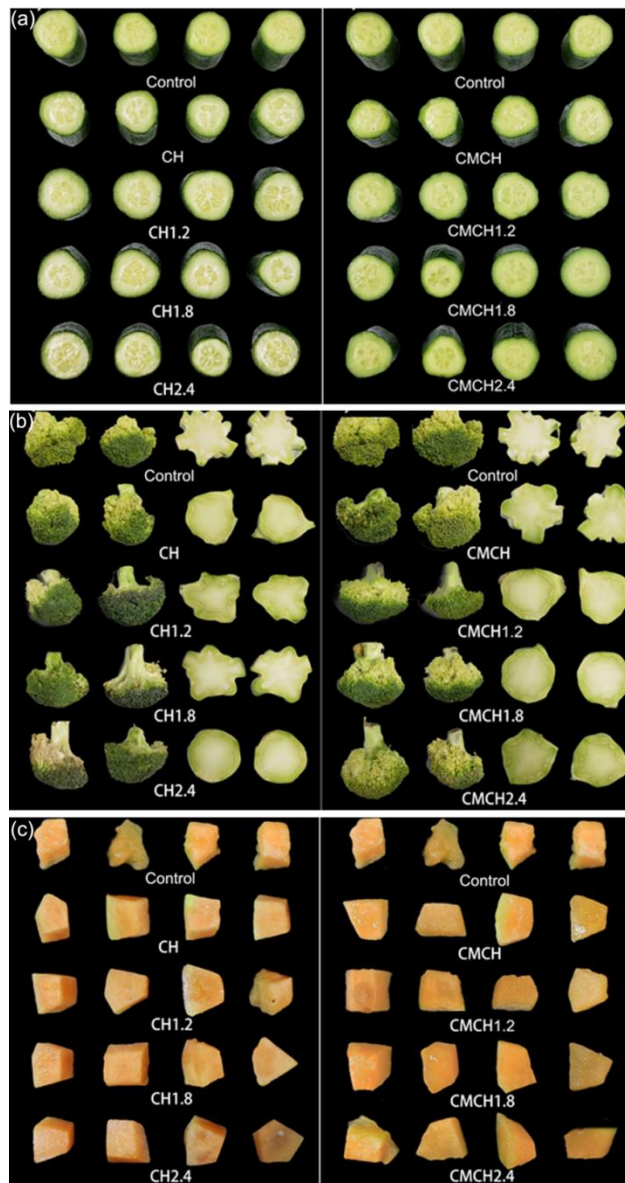
496 Loss of green color of broccoli florets is one of the important factors which influence the
497 quality of post-harvested produce. Takeda et al. (1993) reported more than 80% reduction
498 in chlorophyll in broccoli florets within 4 days when stored at 23 °C. The present study
499 results revealed that coating can effectively attenuate the decrease of chlorophyll
500 concentration. Compared to control, treatment of MLT can mediate the decline of
501 chlorophyll a (Table 2). The level of chlorophyll a in control treatment declined from 4.33
502 $\mu\text{g mg}^{-1}$ on day 0 to 2.93 $\mu\text{g mg}^{-1}$ on day 3. And the level of chlorophyll a in CH1.2 and
503 CH1.8 is 1.95 and 1.89 times higher than control, respectively, manifesting the significant
504 effect of MLT to maintain the color of *Brassica oleracea* ($p<0.05$). These results are in
505 agreement with other studies on coating fresh-cut vegetable samples (María V. Alvarez et
506 al., 2013; Zhang J et al., 2017; Arnao, M.B., Hernández-Ruiz, J, 2009). For instance,
507 Arnao, M.B., Hernández-Ruiz, J (2009) reported that the chlorophyll loss in barley leaves
508 slowed down when treated with MLT. The present results revealed that the quality of
509 postharvest *Brassica oleracea* would be largely retained by the application of MLT. This
510 might be due to the higher antioxidant activity of the MLT film which prevents the
511 chlorophyll degradation.

512 3.4.3 Melon (*Cucumis melo var. saccharinus*)

513 Morphological characteristics of melon were shown in Fig. 8c. In control group, melon
514 showed loss of water and softness of tissue, which prevent them to keep in its original
515 form. However, melon coated with CMLLA had a better appearance and sensory

516 properties. Table 2 showed that the melon quality corresponding to CMLLA. Tissue
517 softening occurs in melons during storage, and associated to the changes in the structure,
518 composition and linkages, which further contributed to its decreased weight and firmness
519 (Li et al., 2013a; Ortiz et al., 2011). Weight loss was declined in case of CMCH1.2 and
520 CMCH1.8, which was 46.19% and 36.11% lower than control, respectively. And firmness
521 in CH1.2 was improved by 9.28 times than control. Fresh-cut melons, as we knew, are
522 prone to quick physiological and microbial deterioration resulted in softening and juice loss
523 (Elena et al., 2018). Similar studies had been reported that coatings physically enhanced
524 the structure of melon and slowed down their degradation (Baldwin, Hagenmaier, & Bai,
525 2011). And many researchers had pointed out that coating with chitosan could effectively
526 prevented weight loss due to a stable and uniform barrier created by chitosan coatings
527 (Kader, 2002; Ochoa-Velasco et al., 2014; Ali et al., 2011).

528 TSS under different treatments showed significant differences ($p < 0.05$). Coating groups
529 had significantly higher TSS values when compared with control groups. The level of TSS
530 in the control group was declined from 16.32% to 11.43%. And low concentration (1.2%,
531 1.8%) CH showed TSS 1.23 and 1.25 times higher than control, respectively. The similar
532 results of MLT coating on fresh-cut fruits were reported elsewhere (Gao et al., 2016; Ma et
533 al., 2016; Liu et al., 2018; Liu et al., 2016). For instance, Liu et al. (2016) reported tomato
534 fruits treated with MLT have higher soluble solid and sugar contents than control. These
535 results indicated that MLT can increase fruits ability to resist oxidative stress and then
536 delay postharvest senescence (Ma et al., 2016). Results showed that under treatment of
537 MLT-incorporated assembly, sensory properties of melon would be largely maintained and
538 decrease of TSS would be retarded.



539

540

Fig. 8. Impact of CMLLA on morphological characteristics of fresh products

Table 3. CMLLA on quality attributes of *Cucumis sativus*, *Brassica oleracea*, and *Cucumis melo* (average \pm standard deviation)

CH						CMCH					
<i>Cucumis sativus</i>	Weight loss /%	Firmness /g		Sugar-acid ratio	ΔE	Weight loss /%	Firmness /g		Sugar-acid ratio	ΔE	
		Section of fruit	Section of center				Section of fruit	Section of center			
Control	18.81 \pm 3.33 ^{b*}	1322.83 \pm 35.73 ^a	344.87 \pm 34.50 ^b	1.15 \pm 0.12 ^a	7.72 \pm 0.81 ^c	18.81 \pm 3.33 ^b	1322.83 \pm 35.73 ^a	344.87 \pm 34.50 ^a	1.15 \pm 0.12 ^a	7.72 \pm 0.81 ^b	
CH/CMCH	16.32 \pm 0.76 ^b	2075.83 \pm 22.37 ^c	425.00 \pm 12.59 ^c	1.49 \pm 0.06 ^{bc}	6.48 \pm 0.60 ^a	19.02 \pm 2.04 ^b	1914.37 \pm 92.55 ^a	499.58 \pm 36.01 ^a	1.37 \pm 0.03 ^b	6.62 \pm 0.79 ^{ab}	
C1.2 [#]	10.80 \pm 0.70 ^a	2157.20 \pm 33.46 ^c	631.63 \pm 90.08 ^c	1.58 \pm 0.09 ^c	4.72 \pm 0.35 ^b	12.35 \pm 0.83 ^a	1955.10 \pm 62.81 ^b	440.67 \pm 11.36 ^a	1.74 \pm 0.08 ^c	6.10 \pm 0.40 ^a	
C1.8	11.58 \pm 0.84 ^a	2210.33 \pm 149.26 ^c	467.33 \pm 24.91 ^c	1.41 \pm 0.04 ^b	5.11 \pm 0.63 ^b	11.33 \pm 0.42 ^a	1943.37 \pm 17.06 ^a	657.80 \pm 120.72 ^b	1.50 \pm 0.03 ^b	7.37 \pm 0.28 ^b	
C2.4	17.06 \pm 0.68 ^b	1576.43 \pm 101.11 ^b	405.23 \pm 61.81 ^a	1.47 \pm 0.16 ^{bc}	7.57 \pm 0.87 ^c	13.01 \pm 0.97 ^a	1038.93 \pm 14.09 ^a	293.27 \pm 148.34 ^a	1.16 \pm 0.17 ^a	7.45 \pm 0.59 ^b	

<i>Brassica oleracea</i>	Firmness /g	Chlorophyll concentration				ΔE	Firmness /g	Chlorophyll concentration				ΔE
		Weight loss /%		/mg/L				Weight loss /%		/mg/L		
		Flower	Stem	Chlorophyll a	Chlorophyll b			Flower	Stem	Chlorophyll a	Chlorophyll b	
Control	2548.80 \pm 121.57 ^a	32.54 \pm 4.26 ^b	18.64 \pm 0.29 ^c	2.93 \pm 0.13 ^a	2.54 \pm 0.23 ^a	6.86 \pm 0.19 ^b	2548.80 \pm 121.57 ^a	32.54 \pm 4.26 ^c	18.64 \pm 0.29 ^b	2.93 \pm 0.13 ^a	2.54 \pm 0.23 ^a	6.86 \pm 0.19 ^b
CH/CMCH	3578.90 \pm 88.57 ^b	23.40 \pm 4.01 ^a	19.31 \pm 0.98 ^c	3.21 \pm 0.06 ^b	2.45 \pm 0.10 ^a	6.50 \pm 1.34 ^b	3768.03 \pm 77.25 ^c	26.81 \pm 3.52 ^b	16.82 \pm 2.88 ^b	3.25 \pm 0.18 ^b	2.88 \pm 0.26 ^a	6.09 \pm 1.04 ^b
C1.2	3859.27 \pm 50.20 ^c	24.42 \pm 2.91 ^a	12.89 \pm 1.07 ^{ab}	5.72 \pm 0.09 ^c	3.78 \pm 0.26 ^b	4.03 \pm 0.56 ^a	4392.10 \pm 146.14 ^d	16.64 \pm 2.54 ^a	11.93 \pm 0.36 ^a	4.19 \pm 0.25 ^d	3.98 \pm 0.26 ^b	3.96 \pm 0.83 ^a
C1.8	3397.30 \pm 165.25 ^b	22.38 \pm 4.00 ^a	10.72 \pm 0.28 ^a	5.55 \pm 0.13 ^c	4.12 \pm 0.27 ^b	3.07 \pm 0.90 ^a	3722.80 \pm 182.94 ^c	16.69 \pm 2.19 ^a	10.07 \pm 1.32 ^a	3.72 \pm 0.03 ^c	3.69 \pm 0.06 ^b	2.93 \pm 0.61 ^a
C2.4	3427.73 \pm 152.29 ^b	40.79 \pm 6.72 ^c	14.62 \pm 1.94 ^b	2.99 \pm 0.15 ^a	2.43 \pm 0.26 ^a	4.39 \pm 0.21 ^a	3060.17 \pm 310.54 ^b	19.12 \pm 2.61 ^a	14.00 \pm 1.55 ^{ab}	3.79 \pm 0.08 ^c	2.72 \pm 0.18 ^a	9.55 \pm 1.12 ^c

<i>Cucumis melo</i>	Firmness /g	TSS /%	Weight loss %	ΔE	Firmness /g	TSS /%	Weight loss /%	ΔE
CH/CMCH	253.13 \pm 65.14 ^b	11.90 \pm 0.24 ^a	23.71 \pm 4.14 ^{ab}	10.51 \pm 0.53 ^c	451.83 \pm 56.92 ^b	11.23 \pm 0.59 ^a	25.23 \pm 3.76 ^b	8.74 \pm 0.79 ^b
C1.2	622.00 \pm 40.62 ^d	14.13 \pm 0.17 ^c	15.90 \pm 2.79 ^a	5.60 \pm 0.41 ^a	820.63 \pm 45.59 ^d	15.23 \pm 0.09 ^c	15.68 \pm 2.62 ^a	5.27 \pm 0.90 ^a
C1.8	690.60 \pm 12.34 ^d	14.10 \pm 0.33 ^c	18.88 \pm 6.06 ^a	4.61 \pm 0.49 ^a	814.20 \pm 16.26 ^d	13.43 \pm 0.05 ^b	20.32 \pm 4.41 ^{ab}	7.10 \pm 0.72 ^{ab}
C2.4	410.27 \pm 26.26 ^c	12.90 \pm 0.16 ^b	21.43 \pm 0.98 ^{ab}	8.06 \pm 0.50 ^b	543.60 \pm 16.90 ^c	12.97 \pm 0.37 ^b	22.14 \pm 5.43 ^{ab}	8.65 \pm 1.54 ^b

[#]C1.2 means CH/CMCH1.2; C1.8 means CH/CMCH1.8; C2.4 means CH/CMCH2.4.

*Different superscripts (a-d) within a column indicate significant differences among samples ($p < 0.05$)

542 **4. Conclusions**

543 In the present study, the novel CMLLA was successfully developed and the improved
544 antioxidant and antimicrobial properties of incorporated melatonin were presented.
545 Among all prepared samples, the CMLLA system loading 1.2% CH, 0.8% CMC, and
546 50mg/L MLT was potentially applied in fresh products. Incorporation of CMC and MLT
547 greatly improved the mechanical strength (increased by 100%), opacity; while the water
548 barrier property was enhanced. Structural characterization further verified the
549 compatibility of the component polymers and improved properties were ascribed to the
550 cross-linking interaction between CMC and chitosan. Besides, CMLLA was also shown
551 antioxidant and antimicrobial activities. Moreover, results from the present study
552 demonstrated the practical applicability of the developed CMLLA on fresh-cut cucumbers,
553 broccolis and melons by maintaining the quality attributes including firmness, total soluble
554 solid and chlorophyll contents; while preventing the weight loss and color degradation.
555 Conclusively, the improvement of mechanical strength and morphological characteristics
556 of CMLLA indicated that the chitosan incorporated with MLT and CMC was potentially
557 applied in maintaining post-harvest quality of fresh products, although further research is
558 essential to evaluate the safety of the CMLLA system before commercialization.
559

- 561 Aghdam, M. S., & Fard, J. R. (2017). Melatonin treatment attenuates postharvest decay and
562 maintains nutritional quality of strawberry fruits (*Fragaria × anannasa* cv. *Selva*) by
563 enhancing GABA shunt activity. *Food Chemistry*, 221, 1650–1657. [https://doi.org/10](https://doi.org/10.1016/j.foodchem.2016.10.123)
564 [.1016/j.foodchem.2016.10.123](https://doi.org/10.1016/j.foodchem.2016.10.123)
- 565 Aider, M. (2010). Chitosan application for active bio-based films production and potential in the
566 food industry: Review. *LWT - Food Science and Technology*, 43(6), 837–842.
567 <https://doi.org/10.1016/j.lwt.2010.01.021>
- 568 Ali, A., Muhammad, M. T. M., Sijam, K., & Siddiqui, Y. (2011). Effect of chitosan coatings on the
569 physicochemical characteristics of Eksotika II papaya (*Carica papaya* L.) fruit during cold
570 storage. *Food Chemistry*, 124(2), 620–626. [https://doi.org/10.1016/j.foodchem.2](https://doi.org/10.1016/j.foodchem.2010.06.085)
571 [010.06.085](https://doi.org/10.1016/j.foodchem.2010.06.085)
- 572 Aljawish, A., Muniglia, L., Klouj, A., Jasniewski, J., Scher, J., & Desobry, S. (2016).
573 Characterization of films based on enzymatically modified chitosan derivatives with
574 phenol compounds. *Food Hydrocolloids*, 60, 551–558. [https://doi.org/10.1016/j.foodhyd](https://doi.org/10.1016/j.foodhyd.2016.04.032)
575 [.2016.04.032](https://doi.org/10.1016/j.foodhyd.2016.04.032)
- 576 Alvarez, M. V., Ponce, A. G., & Moreira, M. del R. (2013). Antimicrobial efficiency of chitosan
577 coating enriched with bioactive compounds to improve the safety of fresh cut broccoli.
578 *LWT - Food Science and Technology*, 50(1), 78–87. [https://doi.org/10.1016/j.lwt.2012](https://doi.org/10.1016/j.lwt.2012.06.021)
579 [.06.021](https://doi.org/10.1016/j.lwt.2012.06.021)
- 580 Arnao, M. B., & Hernández-Ruiz, J. (2017). Melatonin and its relationship to plant hormones.
581 *Annals of Botany*, 121(2), 195–207. <https://doi.org/10.1093/aob/mcx114>
- 582 Arnao, M., & Hernández-Ruiz, J. (2008). Protective effect of melatonin against chlorophyll
583 degradation during the senescence of barley leaves. *Journal of Pineal Research*, 46,
584 58–63. <https://doi.org/10.1111/j.1600-079X.2008.00625.x>
- 585 Bao, D., Chen, M., Wang, H., Wang, J., Liu, C., & Sun, R. (2014). Preparation and
586 characterization of double crosslinked hydrogel films from carboxymethylchitosan and
587 carboxymethylcellulose. *Carbohydrate Polymers*, 110, 113–120. [https://doi.org/10.1016/j.](https://doi.org/10.1016/j.carbpol.2014.03.095)
588 [carbpol.2014.03.095](https://doi.org/10.1016/j.carbpol.2014.03.095)
- 589 Blažević, F., Milekić, T., Romić, M. D., Juretić, M., Pepić, I., Filipović-Grčić, J., ... Hafner, A.
590 (2016). Nanoparticle-mediated interplay of chitosan and melatonin for improved wound
591 epithelialisation. *Carbohydrate Polymers*, 146, 445–454. [https://doi.org/10.1016/j.carbpol](https://doi.org/10.1016/j.carbpol.2016.03.074)
592 [.2016.03.074](https://doi.org/10.1016/j.carbpol.2016.03.074)
- 593 Boy, R., Maness, C., & Kotek, R. (2015). Properties of Chitosan/Soy Protein Blended Films
594 with Added Plasticizing Agent as a Function of Solvent Type at Acidic pH. *International*
595 *Journal of Polymeric Materials and Polymeric Biomaterials*, 65, 150923085124007.
596 <https://doi.org/10.1080/00914037.2015.1038821>
- 597 Branca, C., D'Angelo, G., Crupi, C., Khouzami, K., Rifici, S., Ruello, G., & Wanderlingh, U.
598 (2016). Role of the OH and NH vibrational groups in polysaccharide-nanocomposite
599 interactions: A FTIR-ATR study on chitosan and chitosan/clay films. *Polymer*, 99,
600 614–622. <https://doi.org/10.1016/j.polymer.2016.07.086>
- 601 Brink, I., Šipailienė, A., & Leskauskaitė, D. (2019). Antimicrobial properties of chitosan and
602 whey protein films applied on fresh cut turkey pieces. *International Journal of Biological*
603 *Macromolecules*, 130, 810–817. <https://doi.org/10.1016/j.ijbiomac.2019.03.021>
- 604 Chao, Z., Yue, M., Xiaoyan, Z., & Dan, M. (2010). Development of Soybean Protein-Isolate
605 Edible Films Incorporated with Beeswax, Span 20, and Glycerol. *Journal of Food*
606 *Science*, 75, C493-7. <https://doi.org/10.1111/j.1750-3841.2010.01666.x>
- 607 Chen, C., & Ho, C. (1995). Antioxidant Properties of Polyphenols Extracted from Green and
608 Black Teas. *Journal of Food Lipids*, 2(1), 35–46. [https://doi.org/10.1111/j.1745-4522.1](https://doi.org/10.1111/j.1745-4522.1995.tb00028.x)
609 [995.tb00028.x](https://doi.org/10.1111/j.1745-4522.1995.tb00028.x)
- 610 Chen, W., Li, Y., Yang, S., Yue, L., Jiang, Q., & Xia, W. (2015). Synthesis and antioxidant
611 properties of chitosan and carboxymethyl chitosan-stabilized selenium nanoparticles.

612 *Carbohydrate Polymers*, 132, 574–581. <https://doi.org/10.1016/j.carbpol.2015.06.064>
613 Chen, X., Lee, C. M., & Park, H. (2003). O/W Emulsification for the Self-Aggregation and
614 Nanoparticle Formation of Linoleic Acid Modified Chitosan in the Aqueous System.
615 *Journal of Agricultural and Food Chemistry*, 51(10), 3135–3139. [https://doi.org/10.1021](https://doi.org/10.1021/jf0208482)
616 [/jf0208482](https://doi.org/10.1021/jf0208482)
617 Chung, Y. C., & Chen, C. Y. (2008). Antibacterial characteristics and activity of acid-soluble
618 chitosan. *Bioresource Technology*, 99(8), 2806–2814. <https://doi.org/10.1016/j.biortech.2007.06.044>
619
620 de Abreu, F. R., & Campana-Filho, S. P. (2009). Characteristics and properties of
621 carboxymethylchitosan. *Carbohydrate Polymers*, 75(2), 214–221. [https://doi.org/10.](https://doi.org/10.1016/j.carbpol.2008.06.009)
622 [1016/j.carbpol.2008.06.009](https://doi.org/10.1016/j.carbpol.2008.06.009)
623 de Moraes Crizel, T., de Oliveira Rios, A., D. Alves, V., Bandarra, N., Moldão-Martins, M., &
624 Hickmann Flôres, S. (2018). Active food packaging prepared with chitosan and olive
625 pomace. *Food Hydrocolloids*, 74, 139–150. [https://doi.org/10.1016/j.foodhyd.](https://doi.org/10.1016/j.foodhyd.2017.08.007)
626 [2017.08.007](https://doi.org/10.1016/j.foodhyd.2017.08.007)
627 Esteghlal, S., Niakousari, M., & Hosseini, S. M. H. (2018). Physical and mechanical properties
628 of gelatin-CMC composite films under the influence of electrostatic interactions.
629 *International Journal of Biological Macromolecules*, 114, 1–9. [https://doi.org/10.1016/j.ij](https://doi.org/10.1016/j.ijbiomac.2018.03.079)
630 [biomac.2018.03.079](https://doi.org/10.1016/j.ijbiomac.2018.03.079)
631 Farshi Azhar, F., & Olad, A. (2014). A study on sustained release formulations for oral delivery
632 of 5-fluorouracil based on alginate–chitosan/montmorillonite nanocomposite systems.
633 *Applied Clay Science*, 101, 288–296. <https://doi.org/10.1016/j.clay.2014.09.004>
634 Feng, F., Liu, Y., Zhao, B., & Hu, K. (2012). Characterization of half N-acetylated chitosan
635 powders and films. *2011 Chinese Materials Conference*, 27, 718–732. [https://doi.org](https://doi.org/10.1016/j.proeng.2011.12.511)
636 [/10.1016/j.proeng.2011.12.511](https://doi.org/10.1016/j.proeng.2011.12.511)
637 Fernandez-Saiz, P., Lagaron, J. M., & Ocio, M. J. (2009). Optimization of the biocide
638 properties of chitosan for its application in the design of active films of interest in the food
639 area. *Food Hydrocolloids*, 23(3), 913–921. <https://doi.org/10.1016/j.foodhyd.2008.06.001>
640 Fernández-Saiz, P., Sánchez, G., Soler, C., Lagaron, J. M., & Ocio, M. J. (2013). Chitosan
641 films for the microbiological preservation of refrigerated sole and hake fillets. *Food*
642 *Control*, 34(1), 61–68. <https://doi.org/10.1016/j.foodcont.2013.03.047>
643 Gao, H., Zhang, Z. K., Chai, H. K., Cheng, N., Yang, Y., Wang, D. N., Cao, W. (2016).
644 Melatonin treatment delays postharvest senescence and regulates reactive oxygen
645 species metabolism in peach fruit. *Postharvest Biology and Technology*, 118, 103–110.
646 <https://doi.org/10.1016/j.postharvbio.2016.03.006>
647 Gennadios, A., Hanna, M. A., & Kurth, L. B. (1997). Application of Edible Coatings on Meats,
648 Poultry and Seafoods: A Review. *LWT - Food Science and Technology*, 30(4), 337–350.
649 <https://doi.org/10.1006/fstl.1996.0202>
650 Ghasemzadeh, H., Mahboubi, A., Karimi, K., & Hassani, S. (2016). Full polysaccharide
651 chitosan-CMC membrane and silver nanocomposite: Synthesis, characterization, and
652 antibacterial behaviors. *Polymers for Advanced Technologies*, 27, n/a-n/a. [https://doi.or](https://doi.org/10.1002/pat.3785)
653 [g/10.1002/pat.3785](https://doi.org/10.1002/pat.3785)
654 Guo, Z., Xing, R., Liu, S., Yu, H., Wang, P., Li, C., & Li, P. (2005). The synthesis and
655 antioxidant activity of the Schiff bases of chitosan and carboxymethyl chitosan.
656 *Bioorganic & Medicinal Chemistry Letters*, 15(20), 4600–4603. [https://doi.org/10.1016/j](https://doi.org/10.1016/j.bmcl.2005.06.095)
657 [.bmcl.2005.06.095](https://doi.org/10.1016/j.bmcl.2005.06.095)
658 Huang, Y., Wang, Y. J., Wang, Y., Yi, S., Fan, Z., Sun, L., Zhang, M. (2015). Exploring naturally
659 occurring ivy nanoparticles as an alternative biomaterial. *Acta Biomaterialia*, 25, 268–283.
660 <https://doi.org/10.1016/j.actbio.2015.07.035>
661 Jeon, Y. (2001). Antimicrobial effect of chitooligosaccharides produced by bioreactor.
662 *Carbohydrate Polymers*, 44(1), 71–76. [https://doi.org/10.1016/S0144-8617\(00\)00200-9](https://doi.org/10.1016/S0144-8617(00)00200-9)
663 Kader, A. (2002). Quality Parameters of Fresh-cut Fruit and Vegetable Products. In *Fresh-Cut*

664 *Fruits and Vegetables: Science, Technology, and Market.* <https://doi.org/10.1201/978>
665 [1420031874.ch2](https://doi.org/10.1201/9781420031874.ch2)

666 Kennedy, R., Costain, D. J., McAlister, V. C., & Lee, T. D. G. (1996). Prevention of experimental
667 postoperative peritoneal adhesions by N,O-carboxymethyl chitosan. *Surgery*, 120(5),
668 866–870. [https://doi.org/10.1016/S0039-6060\(96\)80096-1](https://doi.org/10.1016/S0039-6060(96)80096-1)

669 Kritchenkov, A. S., Egorov, A. R., Kurasova, M. N., Volkova, O. V., Meledina, T. V., Lipkan, N.
670 A., dos Santos, W. M. (2019). Novel non-toxic high efficient antibacterial azido chitosan
671 derivatives with potential application in food coatings. *Food Chemistry*, 301, 125247.
672 <https://doi.org/10.1016/j.foodchem.2019.125247>

673 Kucukgulmez, A., Celik, M., Yanar, Y., Sen, D., Polat, H., & Kadak, A. E. (2011).
674 Physicochemical characterization of chitosan extracted from *Metapenaeus stebbingi*
675 shells. *Food Chemistry*, 126(3), 1144–1148. <https://doi.org/10.1016/j.foodchem.2010>
676 [.11.148](https://doi.org/10.1016/j.foodchem.2010.11.148)

677 Kurek, M., Guinault, A., Voilley, A., Galić, K., & Debeaufort, F. (2014). Effect of relative humidity
678 on carvacrol release and permeation properties of chitosan based films and coatings.
679 *Special Issue: 7th International Conference on Water in Food*, 144, 9–17. <https://doi.org/10.1016/j.foodchem.2012.11.132>

680

681 Lee, S., Han, J., & Han, J. (2015). Development and Evaluation of Apple Peel- and
682 Carboxymethylcellulose-Based Biodegradable Films with Antioxidant and Antimicrobial
683 Properties. *Journal of Food Safety*, 36, n/a-n/a. <https://doi.org/10.1111/jfs.12246>

684 Li, F. X., Ma, B. X., He, Q. H., Lü, C., Wang, B., & Tian, H. (2013). Non-destructive Detection of
685 Firmness of Hami Melon by Hyperspectral Imaging Technique. *Guangzi Xuebao/Acta*
686 *Photonica Sinica*, 42, 592–595. <https://doi.org/10.3788/gzxb20134>
687 [205.0592](https://doi.org/10.3788/gzxb20134.205.0592)

688 Li, K., Zhu, J., Guan, G., & Wu, H. (2019). Preparation of chitosan-sodium alginate films
689 through layer-by-layer assembly and ferulic acid crosslinking: Film properties,
690 characterization, and formation mechanism. *International Journal of Biological*
691 *Macromolecules*, 122, 485–492. <https://doi.org/10.1016/j.ijbiomac.2018.10.188>

692 Lin, L., Xue, L., Durairasan, S., & Haiying, C. (2018). Preparation of ϵ -polylysine/chitosan
693 nanofibers for food packaging against *Salmonella* on chicken. *Food Packaging and Shelf*
694 *Life*, 17, 134–141. <https://doi.org/10.1016/j.fpsl.2018.06.013>

695 Liu, C., Zheng, H., Sheng, K., Liu, W., & Zheng, L. (2018). Effects of melatonin treatment on
696 the postharvest quality of strawberry fruit. *Postharvest Biology and Technology*, 139,
697 47–55. <https://doi.org/10.1016/j.postharvbio.2018.01.016>

698 Liu, Jianlong, Zhang, R., Sun, Y., Liu, Z., Jin, W., & Sun, Y. (2016). The beneficial effects of
699 exogenous melatonin on tomato fruit properties. *Scientia Horticulturae*, 207, 14–20.
700 <https://doi.org/10.1016/j.scienta.2016.05.003>

701 Liu, Jun, Liu, S., Chen, Y., Zhang, L., Kan, J., & Jin, C. (2017). Physical, mechanical and
702 antioxidant properties of chitosan films grafted with different hydroxybenzoic acids. *Food*
703 *Hydrocolloids*, 71, 176–186. <https://doi.org/10.1016/j.foodhyd.2017.05.019>

704 Liu, Jun, Meng, C., Liu, S., Kan, J., & Jin, C. (2017). Preparation and characterization of
705 protocatechuic acid grafted chitosan films with antioxidant activity. *Food Hydrocolloids*,
706 63, 457–466. <https://doi.org/10.1016/j.foodhyd.2016.09.035>

707 Liu, Y., Cai, Y., Jiang, X., Wu, J., & Le, X. (2016). Molecular interactions, characterization and
708 antimicrobial activity of curcumin–chitosan blend films. *Food Hydrocolloids*, 52, 564–572.
709 <https://doi.org/10.1016/j.foodhyd.2015.08.005>

710 Ma, Q., Zhang, T., Zhang, P., & Wang, Z. (2016). Melatonin attenuates postharvest
711 physiological deterioration of cassava storage roots. *Journal of Pineal Research*, 60,
712 n/a-n/a. <https://doi.org/10.1111/jpi.12325>

713 Malafaya, P. B., Silva, G. A., & Reis, R. L. (2007). Natural–origin polymers as carriers and
714 scaffolds for biomolecules and cell delivery in tissue engineering applications. *Advanced*
715 *Drug Delivery Reviews*, 59(4–5), 207–233. <https://doi.org/10.1016/j.addr.2007.03.012>

716 Martins, J. T., Cerqueira, M. A., & Vicente, A. A. (2012). Influence of α -tocopherol on
717 physicochemical properties of chitosan-based films. *Food Hydrocolloids*, 27(1), 220–227.
718 <https://doi.org/10.1016/j.foodhyd.2011.06.011>

719 Mathew, S., & Abraham, T. E. (2008). Characterisation of ferulic acid incorporated
720 starch–chitosan blend films. *Food Hydrocolloids*, 22(5), 826–835. [https://doi.org/10.](https://doi.org/10.1016/j.foodhyd.2007.03.012)
721 [1016/j.foodhyd.2007.03.012](https://doi.org/10.1016/j.foodhyd.2007.03.012)

722 Matinfar, M., Mesgar, A. S., & Mohammadi, Z. (2019). Evaluation of physicochemical,
723 mechanical and biological properties of chitosan/carboxymethyl cellulose reinforced with
724 multiphasic calcium phosphate whisker-like fibers for bone tissue engineering. *Materials*
725 *Science and Engineering: C*, 100, 341–353. <https://doi.org/10.1016/j.msec.2019.03.015>

726 Mayachiew, P., & Devahastin, S. (2010). Effects of drying methods and conditions on release
727 characteristics of edible chitosan films enriched with Indian gooseberry extract. *Food*
728 *Chemistry*, 118(3), 594–601. <https://doi.org/10.1016/j.foodchem.2009.05.027>

729 Meng, J. F., Xu, T. F., Wang, Z., Fang, Y., Xi, Z., & Zhang, Z. (2014). The ameliorative effects of
730 exogenous melatonin on grape cuttings under water-deficient stress: Antioxidant
731 metabolites, leaf anatomy, and chloroplast morphology. *Journal of Pineal Research*, 57.
732 <https://doi.org/10.1111/jpi.12159>

733 Noronha, C. M., de Carvalho, S. M., Lino, R. C., & Barreto, P. L. M. (2014). Characterization of
734 antioxidant methylcellulose film incorporated with α -tocopherol nanocapsules. *Food*
735 *Chemistry*, 159, 529–535. <https://doi.org/10.1016/j.foodchem.2014.02.159>

736 Ochoa-Velasco, C. E., & Guerrero-Beltrán, J. Á. (2014). Postharvest quality of peeled prickly
737 pear fruit treated with acetic acid and chitosan. *Postharvest Biology and Technology*, 92,
738 139–145. <https://doi.org/10.1016/j.postharvbio.2014.01.023>

739 Ohlemiller, K. K., & Frisina, R. D. (2008). Age-Related Hearing Loss and Its Cellular and
740 Molecular Bases. In J. Schacht, A. N. Popper, & R. R. Fay (Eds.), *Auditory Trauma,*
741 *Protection, and Repair* (pp. 145–194). https://doi.org/10.1007/978-0-387-72561-1_6

742 Okuyama, K., Noguchi, K., Kanenari, M., Egawa, T., Osawa, K., & Ogawa, K. (2000).
743 Structural diversity of chitosan and its complexes. *Carbohydrate Polymers*, 41(3),
744 237–247. [https://doi.org/10.1016/S0144-8617\(99\)00142-3](https://doi.org/10.1016/S0144-8617(99)00142-3)

745 Ortiz, A., Graell, J., & Lara, I. (2011). Preharvest calcium applications inhibit some cell
746 wall-modifying enzyme activities and delay cell wall disassembly at commercial harvest
747 of ‘Fuji Kiku-8’ apples. *Postharvest Biology and Technology*, 62(2), 161–167.
748 <https://doi.org/10.1016/j.postharvbio.2011.04.014>

749 Park, H., Choi, B., Hu, J., & Lee, M. (2013). Injectable chitosan hyaluronic acid hydrogels for
750 cartilage tissue engineering. *Acta Biomaterialia*, 9(1), 4779–4786. [https://doi.org/10.1](https://doi.org/10.1016/j.actbio.2012.08.033)
751 [016/j.actbio.2012.08.033](https://doi.org/10.1016/j.actbio.2012.08.033)

752 Portes, E., Gardrat, C., Castellan, A., & Coma, V. (2009). Environmentally friendly films based
753 on chitosan and tetrahydrocurcuminoid derivatives exhibiting antibacterial and
754 antioxidative properties. *Carbohydrate Polymers*, 76(4), 578–584. [https://doi.org/10](https://doi.org/10.1016/j.carbpol.2008.11.031)
755 [.1016/j.carbpol.2008.11.031](https://doi.org/10.1016/j.carbpol.2008.11.031)

756 Poverenov, E., Arnon-Rips, H., Zaitsev, Y., Bar, V., Danay, O., Horev, B., Rodov, V. (2018).
757 Potential of chitosan from mushroom waste to enhance quality and storability of fresh-cut
758 melons. *Food Chemistry*, 268, 233–241. <https://doi.org/10.1016/j.foodchem.2018.06.045>

759 Qiu, L., Shao, Z., Wang, D., Wang, F., Wang, W., & Wang, J. (2014). Carboxymethyl cellulose
760 lithium (CMC-Li) as a novel binder and its electrochemical performance in lithium-ion
761 batteries. *Cellulose*, 21, 2789–2796. <https://doi.org/10.1007/s10570-014-0274-7>

762 Rivero, S., García, M. A., & Pinotti, A. (2010). Crosslinking capacity of tannic acid in plasticized
763 chitosan films. *Carbohydrate Polymers*, 82(2), 270–276. [https://doi.org/10.1016/j.carb](https://doi.org/10.1016/j.carbpol.2010.04.048)
764 [ol.2010.04.048](https://doi.org/10.1016/j.carbpol.2010.04.048)

765 Romić, M. D., Klarić, M. Š., Lovrić, J., Pepić, I., Cetina-Čižmek, B., Filipović-Grčić, J., & Hafner,
766 A. (2016). Melatonin-loaded chitosan/Pluronic® F127 microspheres as in situ forming
767 hydrogel: An innovative antimicrobial wound dressing. *European Journal of*

768 *Pharmaceutics and Biopharmaceutics*, 107, 67–79. <https://doi.org/10.1016/j.ejpb.201>
769 [6.06.013](https://doi.org/10.1016/j.ejpb.2016.06.013)

770 Rubilar, J. F., Cruz, R. M. S., Silva, H. D., Vicente, A. A., Khmelinskii, I., & Vieira, M. C. (2013).
771 Physico-mechanical properties of chitosan films with carvacrol and grape seed extract.
772 *2nd ISEKI_Food Conference*, 115(4), 466–474. <https://doi.org/10.1016/j.jfoodeng.2>
773 [012.07.009](https://doi.org/10.1016/j.jfoodeng.2012.07.009)

774 Sakurai, K. (2000). Glass transition temperature of chitosan and miscibility of
775 chitosan/poly(*N*-vinyl pyrrolidone) blends. *Polymer*, 41(19), 7051–7056. [https://doi.org/10.](https://doi.org/10.1016/S0032-3861(00)00067-7)
776 [1016/S0032-3861\(00\)00067-7](https://doi.org/10.1016/S0032-3861(00)00067-7)

777 Sánchez-González, L., González-Martínez, C., Chiralt, A., & Cháfer, M. (2010). Physical and
778 antimicrobial properties of chitosan–tea tree essential oil composite films. *Journal of*
779 *Food Engineering*, 98(4), 443–452. <https://doi.org/10.1016/j.jfoodeng.2010.01.026>

780 Sathivel, S. (2005). Chitosan and Protein Coatings Affect Yield, Moisture Loss, and Lipid
781 Oxidation of Pink Salmon (*Oncorhynchus gorbuscha*) Fillets During Frozen Storage.
782 *Journal of Food Science*, 70, e455–e459. [https://doi.org/10.1111/j.1365-2621.2005.](https://doi.org/10.1111/j.1365-2621.2005.tb11514.x)
783 [tb11514.x](https://doi.org/10.1111/j.1365-2621.2005.tb11514.x)

784 Sayari, N., Sila, A., Abdelmalek, B. E., Abdallah, R. B., Ellouz-Chaabouni, S., Bougatef, A., &
785 Balti, R. (2016). Chitin and chitosan from the Norway lobster by-products: Antimicrobial
786 and anti-proliferative activities. *International Journal of Biological Macromolecules*, 87,
787 163–171. <https://doi.org/10.1016/j.ijbiomac.2016.02.057>

788 Seo, S., King, J. M., & Prinyawiwatkul, W. (2007). Simultaneous Depolymerization and
789 Decolorization of Chitosan by Ozone Treatment. *Journal of Food Science*, 72(9),
790 C522–C526. <https://doi.org/10.1111/j.1750-3841.2007.00563.x>

791 Seydim, A. C., & Sarikus, G. (2006). Antimicrobial activity of whey protein based edible films
792 incorporated with oregano, rosemary and garlic essential oils. *Food Research*
793 *International*, 39(5), 639–644. <https://doi.org/10.1016/j.foodres.2006.01.013>

794 Shi, H., Chen, Y., Tan, D. X., Reiter, R., Chan, Z., & He, C. (2015). Melatonin induces nitric
795 oxide and the potential mechanisms relate to innate immunity against bacterial pathogen
796 infection in Arabidopsis. *Journal of Pineal Research*, 59, 102–108. [https://doi.org/10.1111](https://doi.org/10.1111/jpi.12244)
797 [/jpi.12244](https://doi.org/10.1111/jpi.12244)

798 Shi, H., Reiter, R., Tan, D. X., & Chan, Z. (2014). Indole-3-acetic Acid Inducible 17 positively
799 modulates natural leaf senescence through melatonin-mediated pathway in Arabidopsis.
800 *Journal of Pineal Research*, 58, 26–33. <https://doi.org/10.1111/jpi.12188>

801 Siripatrawan, U., & Harte, B. R. (2010). Physical properties and antioxidant activity of an active
802 film from chitosan incorporated with green tea extract. *Food Hydrocolloids*, 24(8),
803 770–775. <https://doi.org/10.1016/j.foodhyd.2010.04.003>

804 Sogut, E., & Seydim, A. C. (2018). Development of Chitosan and Polycaprolactone based
805 active bilayer films enhanced with nanocellulose and grape seed extract. *Carbohydrate*
806 *Polymers*, 195, 180–188. <https://doi.org/10.1016/j.carbpol.2018.04.071>

807 Song, R., Murphy, M., Li, C., Ting, K., Soo, C., & Zheng, Z. (2018). Current development of
808 biodegradable polymeric materials for biomedical applications. *Drug Design,*
809 *Development and Therapy*, 12, 3117–3145. <https://doi.org/10.2147/DDDT.S165440>

810 Soutos, N., Tzikas, Z., Abraham, A., Georgantelis, D., & Ambrosiadis, I. (2008). Chitosan
811 effects on quality properties of Greek style fresh pork sausages. *Meat Science*, 80(4),
812 1150–1156. <https://doi.org/10.1016/j.meatsci.2008.05.008>

813 Sozer, N., & Kokini, J. L. (2009). Nanotechnology and its applications in the food sector.
814 *Trends in Biotechnology*, 27(2), 82–89. <https://doi.org/10.1016/j.tibtech.2008.10.010>

815 Su, J. F., Huang, Z., Yuan, X. Y., Wang, X. Y., & Li, M. (2010). Structure and properties of
816 carboxymethyl cellulose/soy protein isolate blend edible films crosslinked by Maillard
817 reactions. *Carbohydrate Polymers*, 79(1), 145–153. [https://doi.org/10.1016/j.carbpol.20](https://doi.org/10.1016/j.carbpol.2009.07.035)
818 [09.07.035](https://doi.org/10.1016/j.carbpol.2009.07.035)

819 Sun, L., Sun, J., Chen, L., Niu, P., Yang, X., & Guo, Y. (2017). Preparation and characterization

820 of chitosan film incorporated with thinned young apple polyphenols as an active
821 packaging material. *Carbohydrate Polymers*, 163, 81–91. <https://doi.org/10.1016/j.carb>
822 [pol.2017.01.016](https://doi.org/10.1016/j.carbpol.2017.01.016)

823 Sun, Y., Liu, Z., Lan, G., Jiao, C., & Sun, Y. (2019). Effect of exogenous melatonin on
824 resistance of cucumber to downy mildew. *Scientia Horticulturae*, 255, 231–241.
825 <https://doi.org/10.1016/j.scienta.2019.04.057>

826 Takeda, Y., Yoza, K. I., Nogata, Y., & Ohta, H. (1993). Effects of Storage Temperatures on
827 Polyamine Content of Some Leafy Vegetables. *Journal of the Japanese Society for*
828 *Horticultural Science*, 62(2), 425–430. <https://doi.org/10.2503/jjshs.62.425>

829 Tan, D. X., Manchester, L. C., Helton, P., & Reiter, R. J. (2007). Phytoremediative capacity of
830 plants enriched with melatonin. *Plant Signaling & Behavior*, 2(6), 514–516. <https://doi.org/10.4161/psb.2.6.4639>

831

832 Tan, Y. M., Lim, S. H., Tay, B. Y., Lee, M. W., & Thian, E. S. (2015). Functional chitosan-based
833 grapefruit seed extract composite films for applications in food packaging technology. *SI:*
834 *6th ISFM 2014*, 69, 142–146. <https://doi.org/10.1016/j.materresbull.2014.11.041>

835 Tang, X. Z., Kumar, P., Alavi, S., & Sandeep, K. P. (2012). Recent Advances in Biopolymers
836 and Biopolymer-Based Nanocomposites for Food Packaging Materials. *Critical Reviews*
837 *in Food Science and Nutrition*, 52(5), 426–442. [https://doi.org/10.1080/10408398.](https://doi.org/10.1080/10408398.2010.500508)
838 [2010.500508](https://doi.org/10.1080/10408398.2010.500508)

839 Tang, Y., Yang, X., Hang, B., Li, J., Huang, L., Huang, F., & Xu, Z. (2016). Efficient Production
840 of Hydroxylated Human-Like Collagen Via the Co-Expression of Three Key Genes in
841 *Escherichia coli Origami* (DE3). *Applied Biochemistry and Biotechnology*, 178(7),
842 1458–1470. <https://doi.org/10.1007/s12010-015-1959-6>

843 Tekbas, O. F., Ogur, R., Korkmaz, A., Kilic, A., & Reiter, R. J. (2008). Melatonin as an antibiotic:
844 New insights into the actions of this ubiquitous molecule. *Journal of Pineal Research*,
845 44(2), 222–226. <https://doi.org/10.1111/j.1600-079X.2007.00516.x>

846 US FDA (US Food and Drug Administration). Center for Food Safety and Applied Nutrition.
847 Office of Premarket Approval. *GRAS notices received in 2001*. Available at:
848 <http://vm.cfsan.fda.gov>.

849 Van den Broek, L. A. M., Knoop, R. J. I., Kappen, F. H. J., & Boeriu, C. G. (2015). Chitosan
850 films and blends for packaging material. *Carbohydrate Polymers*, 116, 237–242.
851 <https://doi.org/10.1016/j.carbpol.2014.07.039>

852 Vielma, J. R., Bonilla, E., Chacín Bonilla, L., Mora, M., Medina Leendertz, S., & Bravo, Y.
853 (2014). Effects of melatonin on oxidative stress, and resistance to bacterial, parasitic,
854 and viral infections: A review. *Acta Tropica*, 137, 31–38. <https://doi.org/10.1016/j.acta>
855 [tropica.2014.04.021](https://doi.org/10.1016/j.acta tropica.2014.04.021)

856 Wahid, F., Yin, J. J., Xue, D. D., Xue, H., Lu, Y. S., Zhong, C., & Chu, L. Q. (2016). Synthesis
857 and characterization of antibacterial carboxymethyl Chitosan/ZnO nanocomposite
858 hydrogels. *International Journal of Biological Macromolecules*, 88, 273–279.
859 <https://doi.org/10.1016/j.ijbiomac.2016.03.044>

860 Wang, H., Gong, X., Miao, Y., Guo, X., Liu, C., Fan, Y. Y., Li, W. (2019). Preparation and
861 characterization of multilayer films composed of chitosan, sodium alginate and
862 carboxymethyl chitosan-ZnO nanoparticles. *Food Chemistry*, 283, 397–403. <https://doi.org/10.1016/j.foodchem.2019.01.022>

863

864 Wang, K., Lim, P. N., Tong, S. Y., & Thian, E. S. (2019). Development of grapefruit seed
865 extract-loaded poly(ϵ -caprolactone)/chitosan films for antimicrobial food packaging. *Food*
866 *Packaging and Shelf Life*, 22, 100396. [https://doi.org/10.1016/j.fpsl.2019.100396](https://doi.org/10.1016/j.foodchem.2019.01.022)

867 Wang, S. F., Shen, L., Tong, Y. J., Chen, L., Phang, I. Y., Lim, P. Q., & Liu, T. X. (2005).
868 Biopolymer chitosan/montmorillonite nanocomposites: Preparation and characterization.
869 *Polymer Degradation and Stability*, 90(1), 123–131. <https://doi.org/10.1016/j.polym>
870 [degradstab.2005.03.001](https://doi.org/10.1016/j.polym degradstab.2005.03.001)

871 Wang, X., Yong, H., Gao, L., Li, L., Jin, M., & Liu, J. (2019). Preparation and characterization of

872 antioxidant and pH-sensitive films based on chitosan and black soybean seed coat
873 extract. *Food Hydrocolloids*, 89, 56–66. <https://doi.org/10.1016/j.foodhyd.2018.10.019>
874 Wang, Y., Reiter, R., & Chan, Z. (2017). Phytomelatonin: A universal abiotic stress regulator.
875 *Journal of Experimental Botany*, 69. <https://doi.org/10.1093/jxb/erx473>
876 Wu, C., Tian, J., Li, S., Wu, T., Hu, Y., Chen, S., Ye, X. (2016). Structural properties of films and
877 rheology of film-forming solutions of chitosan gallate for food packaging. *Carbohydrate*
878 *Polymers*, 146, 10–19. <https://doi.org/10.1016/j.carbpol.2016.03.027>
879 Xin, D., Si, J., & Kou, L. (2017). Postharvest exogenous melatonin enhances quality and
880 delays the senescence of cucumber. *Acta Horticulturae Sinica*, 44, 891–901. [https://doi.](https://doi.org/10.16420/j.issn.0513-353x.2016-0888)
881 [org/10.16420/j.issn.0513-353x.2016-0888](https://doi.org/10.16420/j.issn.0513-353x.2016-0888)
882 Yan, J., Luo, Z., Ban, Z., Lu, H., Li, D., Yang, D., ... Li, L. (2019). The effect of the
883 layer-by-layer (LBL) edible coating on strawberry quality and metabolites during storage.
884 *Postharvest Biology and Technology*, 147, 29–38. <https://doi.org/10.1016/j.posthar>
885 [vbio.2018.09.002](https://doi.org/10.1016/j.postharvbio.2018.09.002)
886 Yang, H., Yan, R., Chen, H., Lee, D. H., & Zheng, C. (2007). Characteristics of hemicellulose,
887 cellulose and lignin pyrolysis. *Fuel*, 86(12), 1781–1788. <https://doi.org/10.1016/j.fuel>
888 [.2006.12.013](https://doi.org/10.1016/j.fuel.2006.12.013)
889 Yen, M. T., Yang, J. H., & Mau, J. L. (2008). Antioxidant properties of chitosan from crab shells.
890 *Carbohydrate Polymers*, 74(4), 840–844. <https://doi.org/10.1016/j.carbpo>
891 [l.2008.05.003](https://doi.org/10.1016/j.carbpol.2008.05.003)
892 Yu, S. H., Hsieh, H. Y., Pang, J. C., Tang, D. W., Shih, C. M., Tsai, M. L., Mi, F. L. (2013). Active
893 films from water-soluble chitosan/cellulose composites incorporating releasable caffeic
894 acid for inhibition of lipid oxidation in fish oil emulsions. *Food Hydrocolloids*, 32(1), 9–19.
895 <https://doi.org/10.1016/j.foodhyd.2012.11.036>
896 Zhai, L., Bai, Z., Zhu, Y., Wang, B., & Luo, W. (2018). Fabrication of chitosan microspheres for
897 efficient adsorption of methyl orange. *Chinese Journal of Chemical Engineering*, 26(3),
898 657–666. <https://doi.org/10.1016/j.cjche.2017.08.015>
899 Zhang, J., Shi, Y., Zhang, X., Du, H., Xu, B., & Huang, B. (2017). Melatonin suppression of
900 heat-induced leaf senescence involves changes in abscisic acid and cytokinin
901 biosynthesis and signaling pathways in perennial ryegrass (*Lolium perenne* L.).
902 *Environmental and Experimental Botany*, 138, 36–45. <https://doi.org/10.1016/j.envexp>
903 [bot.2017.02.012](https://doi.org/10.1016/j.envexpbot.2017.02.012)
904 Zhao, D., Huang, J., Hu, S., Mao, J., & Mei, L. (2011). Biochemical activities of
905 N,O-carboxymethyl chitosan from squid cartilage. *Carbohydrate Polymers*, 85(4),
906 832–837. <https://doi.org/10.1016/j.carbpol.2011.04.007>
907 Zhao, Q., Qian, J., An, Q., Gao, C., Gui, Z., & Jin, H. (2009). Synthesis and characterization of
908 soluble chitosan/sodium carboxymethyl cellulose polyelectrolyte complexes and the
909 pervaporation dehydration of their homogeneous membranes. *Journal of Membrane*
910 *Science*, 333(1), 68–78. <https://doi.org/10.1016/j.memsci.2009.02.001>
911 Zhuang, C., Jiang, Y., Zhong, Y., Zhao, Y., Deng, Y., Yue, J., Mu, H. (2018). Development and
912 characterization of nano-bilayer films composed of polyvinyl alcohol, chitosan and
913 alginate. *Food Control*, 86, 191–199. <https://doi.org/10.1016/j.foodcont.2017.11.024>
914